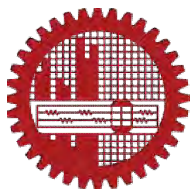


**PREPARATION AND PROPERTIES OF THERMO- AND MAGNETO-  
RESPONSIVE SUPERABSORBENT NANOCOMPOSITE HYDROGEL**

A thesis submitted in partial fulfillment of the requirement  
for the degree of M.Sc. in chemistry

**SUBMITTED BY**

**SALMA SULTANA**  
**STUDENT ID: 1014032702**  
**SESSION: OCTOBER 2014**



**Chemistry Materials Laboratory**  
**Department of Chemistry**  
**Bangladesh University of Engineering and Technology (BUET)**  
**Dhaka-1000, Bangladesh**

**April 2017**

## **DECLARATION BY THE CANDIDATE**

I do hereby declare that this thesis or part of it has not been submitted elsewhere for the award of any degree or diploma.

*Salma sultana .*

.....

**(SALMA SULTANA)**

M.Sc. student

Department of Chemistry

Bangladesh University of Engineering and Technology (BUET)

Dhaka, Bangladesh

**Bangladesh University of Engineering and Technology, Dhaka**  
**Department of Chemistry**



**Certification of Thesis**

**A thesis on**

**PREPARATION AND PROPERTIES OF THERMO- AND MAGNETO-  
RESPONSIVE SUPERABSORBENT NANOCOMPOSITE HYDROGEL**

**BY**

**SALMA SULTANA**

has been accepted as satisfactory in partial fulfillment of the requirements for the degree of Master of Science (M.Sc.) in Chemistry and certify that the student has demonstrated a satisfactory knowledge of the field covered by this thesis in an oral examination held on April 29, 2017.

**Board of Examiners**

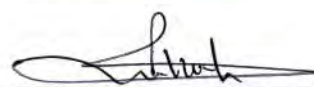
**1. Dr. Md. Shafiqul Azam**  
Assistant Professor  
Department of Chemistry  
BUET, Dhaka



---

Supervisor & Chairman


**2. Dr. Md. Rafique Ullah**  
Professor & Head  
Department of Chemistry  
BUET, Dhaka Member



---

(Ex-officio) 29/04/2017.

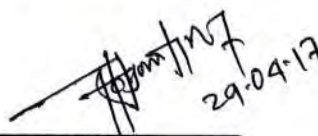
**3. Dr. Shakila Rahman**  
Professor  
Department of Chemistry  
BUET, Dhaka



---

Member

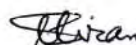
**4. Dr. Md. Shakhawat Hossain Firoz**  
Associate Professor  
Department of Chemistry  
BUET, Dhaka



---

Member

**5. Dr. Muhammed Shah Miran**  
Associate Professor  
Department of Chemistry  
University of Dhaka



---

Member (External)

**Dedicated to**  
**My Honorable Supervisor**  
**&**  
**Beloved Parents**

# Acknowledgement

At the very beginning, I humbly acknowledge my deepest gratitude to the almighty, the most gracious, benevolent and merciful creator for his infinite mercy bestowed on me in carrying out the research work presented in the dissertation.

It is a great pleasure for me to acknowledge my deepest sense of gratitude, sincere, appreciation, heartfelt indebtedness and solemn regards to my reverend teacher and supervisor Dr. Md. Shafiul Azam, Assistant Professor, Department of Chemistry, Bangladesh University of Engineering and Technology (BUET), for his kind supervision, indispensable guidance, valuable and constructive suggestions, liberal help and continuous encouragement during the whole period. It is obvious that his attributive contribution and efforts have greatly shaped me into what I am today. In fact, I am quite lucky to be a part of his ambitious research team.

It is my great honor to convey my sincere gratitude to my respected teacher Professor Dr. Md. Rafique Ullah, honorable Head of the Department of Chemistry, BUET for giving me his wonderful support to move through the academic processes during this M.Sc. program. I would like to convey my deepest gratitude to Professor Dr. Md. Nazrul Islam, Dr. Md. Shakhawat Hossain Firoz, Md. Abu Hasan Howlader, and Dr. Chanchal Kumar Roy, Department of Chemistry, BUET, for their valuable suggestions, appreciated comments, guidance and help during the research period.

I am thankful to all other respected teachers of the Department of Chemistry, BUET, for their time to time support. I would also like to thank all of the officers and staffs of the Department of Chemistry, BUET for their continuous help during my study period.

I am highly thankful to Professor Dr. Hongbo Zeng, University of Alberta, Canada, for the characterization of our samples using X-ray Photoelectron Spectroscopy (XPS) technique during my research.

I am thankful to my dear colleagues Labiba Bushra, Md. Jahangir Hossen for their friendly cooperation and lovely encouragement throughout my research period. Special thanks to Abinash Chandra Roy and Md. Shafiqul Islam, for their continuous help during the research.

I am also thankful to other fellows of Chemistry Materials Laboratory for their cooperation during the research period.

I am grateful to the authority of BUET and The World Academy of Sciences (TWAS) for providing financial support for this research work.

Finally, I would like to express my heartfelt indebtedness and profound gratitude to my beloved father, mother and all of my family members for their continuous inspiration and immeasurable sacrifices throughout the period of my study.

April 2017

Salma Sultana

## Abstract

Hydrogels are highly crosslinked polymer materials that are able to swell when immersed in aqueous solutions. Some hydrogels can be designed in such a way that they undergo some conformational changes in response to external stimuli such as temperature, pH, ionic strength, light, electrical signal and magnetic field etc. The hydrogels have been exploited in a wide variety of applications including drug delivery and tissue engineering, biosensors and microfluidic devices. Herein, we develop a novel strategy for combining thermo- and magneto-responsiveness into one hydrogel system. Specifically, as thermo-sensitive part of the hydrogel we used polyacrylamide, which was crosslinked with acrylic-functionalised silica coated magnetic nanoparticles to possess the magnetic responsiveness.  $\text{Fe}_3\text{O}_4$  nanoparticles were synthesized and coated with silica, which provides the nanoparticles with a reactive surface for functionalization with  $-\text{NH}_2$  group through the silanation with 3-aminopropyl triethoxysilane. The  $-\text{NH}_2$  groups were then further functionalized by reacting with acrylic anhydride to generate magnetic nanoparticles containing acrylic group, which were finally crosslinked with polyacrylamide to give the desired nanocomposite hydrogel. The synthesized nanocomposite was characterized by x-ray photoelectron spectroscopy (XPS), x-ray diffraction (XRD), energy dispersive x-ray (EDX), scanning electron microscopy (SEM), and Fourier transform infrared (FTIR) analysis. The synthesized nanocomposite hydrogel showed thermo-responsive swelling when dipped in water. Interestingly, we observed that a nanocomposite with a certain composition exhibit greater swelling ratio than that of bisacrylamide crosslinked polyacrylamide hydrogel. This swelling ratio decreased with the increase of magnetic crosslinker in the composite hydrogel. On the other hand, the as-synthesized hydrogel showed magnetic behavior owing to the presence magnetite nanoparticles in the form of 3D crosslinker. The prepared nanocomposite hydrogel also exhibited nice self-healing properties due to the presence of  $\text{Fe}_3\text{O}_4$  in the system.

## Contents

Introduction.....	1
1.1 Hydrogel.....	2
1.2 Crosslinker of hydrogel .....	3
1.2.1 One Dimensional Crosslinker .....	3
1.2.2 Two Dimensional Crosslinker.....	4
1.2.3 Three Dimensional Crosslinker.....	4
1.3 Responsiveness of hydrogel .....	5
1.3.1 pH responsive hydrogel.....	5
1.3.2 Thermo-responsive hydrogel.....	5
1.3.3 Magneto- responsive hydrogel .....	6
1.3.4 light responsive hydrogel .....	8
1.3.5 Electric field responsive hydrogel.....	9
1.4 Multi responsive hydrogel .....	10
1.4.1 Magneto- and thermo-responsive hydrogel .....	10
1.4.2 pH- and Thermo-responsive hydrogel .....	10
1.5 Magnetic Nanoparticle synthesis method.....	11
1.5.1 Thermal decomposition method .....	11
1.5.2 Micro emulsion method.....	11
1.5.3 Co-precipitation method .....	11
1.6 Surface modification of Iron oxide nanocomponents.....	11
1.7 Magnetically responsive polymer nanocomponents.....	12
1.8 Thermo-responsive polymer nanocomponents.....	13
1.9. Swelling properties of hydrogel.....	13
1.10 Literature Review .....	14
1.11 Research Goal.....	16
Experimental.....	23
2.1 Materials and Instrument .....	24
2.1.1 Chemicals and Reagents .....	24
2.1.2 Materials .....	24
2.1.3 Instruments .....	25
2.2 Synthesis of magnetic crosslinker .....	25



2.2.1 Synthesis of Fe <sub>3</sub> O <sub>4</sub> .....	25
2.2.2 Silica coated Fe <sub>3</sub> O <sub>4</sub> .....	25
2.2.3 Silica coated Fe <sub>3</sub> O <sub>4</sub> functionalized by –NH <sub>2</sub> group.....	26
2.2.4 Further functionalized by –CH=CH <sub>2</sub> group.....	27
2.3 Synthesis of nanocomposite .....	27
2.4 Swelling study of hydrogel.....	27
2.4.1 Kinetics study of swelling .....	27
2.4.2 Temperature dependent swelling study .....	28
2.5 Self-healing analysis.....	28
2.6 Fourier transform infrared analysis (FTIR) .....	28
2.7 Field emission scanning electron microscopy (SEM) .....	29
2.8 Energy dispersive x-ray (EDX) spectroscopy .....	29
2.9 X-ray diffraction (XRD).....	29
2.10 X-ray photoelectron spectroscopy (XPS).....	30
Results and Discussion .....	32
3.1 Synthesis of magnetic nanocomposite.....	33
3.1.1 Synthesis of magnetic crosslinker .....	33
3.1.2 Polymer nanocomposite Synthesis .....	34
3.2 Functional group analysis using FTIR.....	34
3.3 Swelling measurement.....	37
3.3.1 Kinetics study of swelling .....	37
3.3.2 Temperature dependent swelling study .....	37
3.4 Magnetic test of magnetic crosslinker and hydrogel .....	38
3.5 X-ray photoelectron spectroscopy (XPS).....	39
3.5.1 High Resolution C1s Spectra.....	40
3.5.2 High resolution N1s spectra.....	42
3.6 X-ray diffraction analysis (XRD).....	43
3.7 Surface morphology study using scanning electron microscope (SEM).....	44
3.8 Energy dispersive x-ray spectral analysis.....	49
3.9 Self-healing analysis.....	52
Conclusion .....	53

## List of Figures

Figure 1.1 One dimensional crosslinker .....	3
Figure 1.2 Two dimensional crosslinker .....	4
Figure 1.3 Three dimensional crosslinker .....	4
Figure 1.4 magnetic nanoparticles not covalent bonded .....	16
Figure 1.5 magnetic nanoparticles leave the polymer chain when magnetic field is applied .....	16
Figure: 3.1 Schematic representation of magnetic crosslinker .....	33
Figure 3.2 FTIR spectra of Fe <sub>3</sub> O <sub>4</sub> , silica coated MION, aminated MION and acrylated MION.....	35
Figure 3.3 FTIR spectra of nanocomposite .....	36
Figure 3.4 kinetics study of swelling.....	37
Figure 3.5 Temperature dependent swelling .....	38
Figure 3.6 Magnetic crosslinker dispersed in water and get attract to magnet.....	39
Figure 3.7 polymer nanocomposite hydrogel with magnetic crosslinker is attracted by magnet.....	39
Figure 3.8 Widescan spectra of aminated MION, acrylated MION.....	40
Figure 3.9 High resolution of C1s spectra of aminated MION .....	41
Figure 3.10 High resolution of C1s spectra of acrylated MION .....	41
Figure 3.11 high resolution of N1s spectra of aminated MION .....	42
Figure 3.12 High resolution of N1s spectra of acrylated MION .....	42
Figure 3.13 XRD spectra of Fe <sub>3</sub> O <sub>4</sub> , acrylated MION.....	43
Figure 3.14 XRD spectra of nanocomposite.....	44
Figure 3.15 (A) SEM image of MION at Resolution x 50,000 .....	45
Figure 3.15 (B) SEM image of (MION) at Resolution x 100,000.....	46
Figure 3.17 (A) SEM image of Acrylated MION at Resolution x 50,000 .....	47
Figure 3.17 (B) SEM image of Acrylated MION at Resolution x 100,000.....	47
Figure 3.18 (A) SEM image of nanocomposite (4 : 0.025 g) at Resolution x 50,000.....	48
Figure 3.18 (B) SEM image of nanocomposite at Resolution x 100,000.....	48
Figure 3.19 (A) SEM image of nanocomposite (4: 0.0125 g) at Resolution x 50,000.....	48
Figure 3.19 (B) SEM image of nanocomposite (4: 0.0125 g) at Resolution x 100,000.....	49
Figure 3.20 EDX spectra of Fe <sub>3</sub> O <sub>4</sub> .....	50
Figure 3.21 EDX spectra of silica coated of MION .....	50
Figure 3.22 EDX spectra of acrylated MION.....	51

Figure 3.23(A) EDX spectra of nanocomposite(4:0.0125g) .....52

List of tables

Table 3.1 characteristic IR band of MION, Silica coated MION, Aminated MION, Acrylated MION.....35

Table 3.2 Elemental composition of magnetic and nanocomposite compound.....49

# **Chapter 1**

## **Introduction**

## 1.1 Hydrogel

Hydrogels are highly crosslink polymer materials that are able to swell but do not dissolve in water. The word “hydrogel”, first introduced in 1894 which the material described there was not a hydrogel as we describe it today. It was colloidal gel made with inorganic salts. First generation of hydrogel's that form of a crosslinker involve the chemical of a monomer or polymer with an initiator is to develop material with high swelling, good mechanical properties[1]. Second generation of materials capable of response to specific stimuli, such as temperature, pH, ionic strength, concentration of specific molecules in solution[2]. Finally, a third generation of hydrogels focusing on the investigation and development of stereo complexed materials hydrogels cross linked by other physical interactions. The ability of hydrogels to absorb water arises from hydrophilic functional groups attached to the polymer backbone. The gel is a state that is neither completely liquid nor completely solid. These half liquid-like and half solid-like properties cause many interesting relaxation behaviors that are not found in either a pure solid or a pure liquid.

Hydrogels can be classified into two distinct categories, the natural and the synthetic hydrogels. Natural hydrogels include collagen, fibrin, and derivatives of natural materials such as chitosan, alginate and silk fibers[3]. Two main drawbacks of natural hydrogels, however, make their final microstructures and properties difficult to control re reducibility[4]. In contrast, synthetic hydrogels such as poly (ethylene glycol) di-acrylate, poly-acrylamide, and poly-vinylalcohol are more reproducible, although their final structure can also depend on polymerization conditions. During last two decades, natural hydrogels were gradually replaced by synthetic hydrogels which has long service life, high capacity of water absorption, and high gel strength[5]. Hydrogels can be synthesized from purely synthetic components. Also, it is stable in the conditions of sharp and strong fluctuations of temperatures. Hydrogels may absorb from 10-20% up to thousands of times their dry weight in water. Polymeric hydrogel networks may be formed by various techniques, however the most common synthetic route is the free-radical cross-linking copolymerization of a hydrophilic non-ionic monomer such as acrylamide (AAm) with a small amount of a cross-linker, e.g., N,N'-methylenebisacrylamide (MBAAm). In order to increase their swelling capacity, an ionic monomer is also included into the reaction mixture. Since the monomers for hydrogel preparation are usually solid at the usual polymerization temperature, it is necessary to carry out the polymerization reactions in an

aqueous solution. Hydrogel structure and, thus, the hydrogel properties are closely related to the conditions under which the Hydrogel are formed, i.e., the cross-linker concentration, the initial degree of dilution of the monomers and the chemistry of the units building the network -structure[6]. They possess also a degree of flexibility very similar to natural tissue due to their large water content. Recently, hydrogels have been defined as two or multi-component systems consisting of a three-dimension.

## 1.2 Crosslinker of hydrogel

A cross-link is a bond that links on polymer chain to another. They can be covalent bonds or ionic bonds. Generally, which agents perform this joining work is called crosslinker. Crosslinkers contain at least two reactive groups. Reactive groups that can be targeted for crosslinking include primary amines, sulfhydryls, carbonyls, vinyl group, carbohydrates, carboxylic acids etc. When polymer chains are linked together by cross-linker, they lose some of their ability to move as individual polymer chains. Hence chemical crosslinking is mechanically and thermally stable. Crosslinking may be initiated by heat, pressure, change in pH, or radiation. Crosslinkers are chosen depending on chemical specificity, same or different reactive groups, spontaneously reactive or photo reactive groups etc. Crosslinkers are commonly used to modify nucleic acids, drugs and solid surfaces

### 1.2.1 One Dimensional Crosslinker

In this group of crosslinker the reactive groups are usually remain at the end of chain. It is also called 1D crosslinker. 1D crosslinker contains at least two active sites which are able to react with substrate or polymer matrix. Due to lower active sites comparatively less amount of polymer chains is linked up. Common use linear crosslinkers are N,N'-methylenebisacrylamide(MBA), bis (triethoxysilylpropyl)tetrasulfide, imido ester etc.

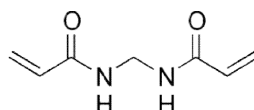


Figure 1.1 One dimensional crosslinker

### 1.2.2 Two Dimensional Crosslinker

Planar cross-linkers are normally called 2D cross-linker. Its reactive groups are on the upper and lower side of the surface. In case of linear crosslinker there are only two linking sites. But in case of 2D crosslinker many more active sites are available on the surface. These active sites interact with the coming group of polymer or other matrices and form an excellent composite material. 2D crosslinkers are able to link comparatively higher number of polymer chains. As a result, different physical and chemical properties are improved by using 2D crosslinker. Well known 2D crosslinkers included nanoclay, graphene oxide (GO) nanoparticles, functionalized GO etc. are widely used to form nanocomposite. These nanocomposites are used in wastewater treatment, electronic devices and many more sectors.



Figure 1.2 Two dimensional crosslinker

### 1.2.3 Three Dimensional Crosslinker

This class of crosslinkers added new dimension in the crosslinked composite materials. The shape of the 3D crosslinker may be spherical. Its surface area is comparatively higher than that of the linear or planar crosslinker. In case of 2D crosslinker only two sides contain active sites for the interaction with substrate but in case of 3D crosslinker, reactive sites are laying all sides of 3D crosslinker. Hence it contains a wide number of reactivitesites in a small surface area.



Figure 1.3 Three dimensional crosslinker

Due to this its reactivity increases dramatically. Since reactive sites are scattered, 3D crosslinkers are able to link with much more polymer chains. As a result of the produced nanocomposite become robust and improved chemical and mechanical properties of the nanocomposites.

### **1.3 Responsiveness of hydrogel**

Typical stimuli are temperature, pH, electric field, light, magnetic field etc. And the responses can also be manifold: dissolution precipitation, degradation, drug release, change in hydration state, swelling/collapsing, hydrophilic/hydrophobic surface, change in shape, conformational change. This article will focus on temperature and magneto as external stimuli, since these systems are predominantly studied. Stimuli-responsive hydrogels are cross-linked, hydrophilic polymer networks that undergo a physicochemical transition in response to a change in external stimuli such as pH, temperature, light and analyte concentration.

#### **1.3.1 pH responsive hydrogel**

pH responsive polymers are materials which will respond to the changes in the pH of the surrounding medium by varying their dimensions. Such materials increase its size (swell) or collapse depending on the pH of their environment. This behavior is exhibited due to the presence of certain functional group in the polymer chain. There are two kinds of pH sensitive materials: one which have acidic group (-COOH, -SO<sub>3</sub>H) and swell in basic pH, and others which have basic groups (-NH<sub>2</sub>) and swell polyacrylic acid is an example of the former chitosan is an example of the latter. The mechanism of response is same for both, only the stimulus varies. In aqueous media of appropriate pH and ionic strength, the pendant groups ionize and develop fixed charges on the polymer network, generating electrostatic repulsive forces responsible for pH dependent swelling or de swelling of the hydrogel, thereby controlling the drug release. Small changes in pH can result in significant change in the mesh size of the polymeric networks.

#### **1.3.2 Thermo-responsive hydrogel**

Thermo-responsive hydrogels are that exhibit a drastic and discontinuous change of their physical properties with temperature. The term is commonly used when the property concerned is solubility in a given, solvent but it may also be used when other properties are



affected. Thermo-responsive polymers belong to the class of stimuli responsive hydrogel, in contrast to temperature-sensitive. Temperature-sensitive hydrogels are probably the most studied class of stimuli sensitive polymer in drug delivery research. These hydrogels are able to swell or de-swell as a result of change in the temperature of the surrounding fluid. Considering volume-phase transitions give us a volume-phase transition temperature (VPTT) instead of a critical solution temperature, there are still two main classifications of observed behavior, positive volume-phase transitions and negative volume-phase transitions. A positive volume-phase transition or “thermophilic” hydrogel will swell upon heating, increasing its volume. A negative volume-phase transition or “thermophobic” hydrogel will collapse upon heating, decreasing its volume. Thermophilic hydrogels typically maintain a collapsed conformation at temperatures below their VPTT while thermophobic hydrogels are able to swell at lower temperatures[7]. Thermo-responsive hydrogels that exhibit a drastic and discontinuous change of their physical properties with temperature. The term is commonly used when the property concerned is solubility in a given solvent but it may also be used when other properties are affected. Thermo-responsive polymers belong to the class of stimuli responsive hydrogel, in contrast to temperature-sensitive.

### **1.3.3 Magneto- responsive hydrogel**

Recently, there is a growing interest and effort to expand the range of available stimuli from temperature, pH which could be limited by mass transfer, to newly emerging remote electromagnetic triggers like light, electricity and magnetic field, to obtain responsive materials with more precise responsivity and higher efficiency. Magnetic nanocomponents are multi-component materials, containing nano sized magnetic materials. They response to an external stimulus i.e., magnetic field, different materials (e.g., gels, liquid crystals, renewable polymers, silica, carbon or metal organic frameworks) with various types of magnetic particles, offering exciting perspectives for fundamental investigation. Magnetic nanomaterials have attracted considerable attention because of their unique size-dependent properties, and many important technological applications. Magnetic nanocomponents usually consist of components exhibiting magnetic properties, like iron oxide such as  $\text{Fe}_3\text{O}_4$  and  $\text{Fe}_2\text{O}_3$ , pure metals such as ferrum Cobalt and nickel, their chemical compounds and alloys. Magnetic properties based on size, shape, structure, crystallinity, and chemistry of materials. In nature iron oxides exist in many forms like magnetite ( $\text{Fe}_3\text{O}_4$ ), hematite ( $\alpha\text{-Fe}_2\text{O}_3$ ) and maghemite ( $\gamma\text{-(Fe}_2\text{O}_3)$ ). Among these oxides  $\text{Fe}_3\text{O}_4$  particles are more

demandable due to surface efficiency. For the first time, the magnetite crystal structure had been studied in 1915 as one of the first mineral structures evaluated through X-ray diffraction method by Bragg and Nishikawa. Recently,  $\text{Fe}_3\text{O}_4$  have been intensively investigated because of their super paramagnetic, high co reactivity and low Curie temperature. Magnetite ( $\text{Fe}_3\text{O}_4$ ) is a kind of excellent magnetic material among iron oxides. It has a cubic inverse spinel structure. which oxygen forms a face centered cubic closed packing and  $\text{Fe}^{3+}$  ions occupy the tetrahedral sites and octahedral sites, and bears distinguished electric and magnetic properties on account of the hopping of electrons between  $\text{Fe}^{2+}$  and  $\text{Fe}^{3+}$  in the octahedral sites. Magnetite has been widely applied in numerous fields such as Ferro fluid, catalysis, pigment color, magnetic storage media, environment protection, cell separation, clinic diagnosis and therapy.  $\text{Fe}_3\text{O}_4$  MNPs are also nontoxic and biocompatible. The name hematite is derived from the Greek word for blood *haima*, due to the red coloration found in some varieties of hematite. Hematite is the form of Iron iron(III) oxide ( $\text{Fe}_2\text{O}_3$ ), hematite exhibits antiferromagnetic behavior below temperature of 260K. This temperature is known as Morin temperature. Above this temperature, hematite exhibits weak ferromagnetic behavior. Hematite is widely used in magnetic recording media, as a catalyst, gas sensors etc. These applications of iron oxide arise due to its low cost, thermal stability, its resistance to corrosion and its non-toxic nature. Among the various magnetic materials, the cubic spinel structured maghemite ( $\gamma\text{-Fe}_2\text{O}_3$ ) represents an important class of magnetic transition metal oxide materials in which oxygen atoms form a face centered close-packed structure.  $\gamma\text{-Fe}_2\text{O}_3$  is an ideal candidate for fabrication of luminescent and magnetic dual functional nanocomposites due to its excellent transparent properties. The existence of amorphous  $\text{Fe}_2\text{O}_3$  and four polymorphs (alpha, beta, gamma and epsilon) is well established. At a temperature of  $650^\circ\text{C}$ , hematite turns into  $\text{Fe}_3\text{O}_4$  with a high energy loss. Hematite has strongly antiferromagnetic properties. Gamma  $\text{Fe}_2\text{O}_3$  (maghemite) is the ferrimagnetic cubic form of Fe(III) oxide and it differs from the inverse spinel structure of magnetite through vacancies on the cation sublattice. In time, at room-temperature, the maghemite turns into hematite crystalline structure. Maghemite has the same crystalline structure like  $\text{Fe}_3\text{O}_4$  (magnetite). Maghemite  $\text{Fe}_2\text{O}_3$  is biocompatible and therefore is one of the most extensively used biomaterials for different applications like cell separation, drug delivery in cancer therapy.

Hydrogels are three dimensional hydrophilic polymer networks that can swell in water and hold a large amount of water while maintaining the structure. A three dimensional

network is formed by crosslinking polymer chains. Crosslinking can be provided by covalent bonds, hydrogen bonding, Vander Waals interactions or physical entanglements. They experience reversible volume changes in response to external stimulus such as pH, temperature and ionic concentration. Stimuli responsive hydrogels often exhibit sharp volume phase transitions triggered by specific chemical or physical stimuli. Volume phase transitions has been vastly studied due to its potential in triggering the functions of movements such as deformation, volume change modulus changes, force generation.

Magneto responsive hydrogel belong to this recent trend and are of special interest, as they can realize temporal and remote control and have great potential, for instance for microfluidic systems in analytical or therapeutic devices.  $\text{Fe}^{3+}$  ions are the most wanted in formation of intracellular and macromolecular biologically active or magnetic resonance contrast materials because of their non-toxicity and their existence in nature in many tissues. For these in vivo applications, the magnetic nanoparticles need to exhibit high magnetic saturation. Biocompatible and non-toxic magnetic nanoparticles, well-dispersed in the solvent carrier, have a lot of potential for in vivo applications in which superparamagnetic particles are of interest because they do not retain any residual magnetism after removal of a magnetic field. Magnetic nanoparticle materials offer major advantages due to their unique size and physicochemical properties. Because of the widespread applications of magnetic nanoparticles in biotechnology, biomedical, material science, engineering, and environmental areas, much attention has been paid to the synthesis of different kinds of magnetic nanoparticles. Other biomedical applications of magnetic nanoparticles include drug delivery and magnetic resonance imaging. The large surface-to-volume ratio of MNPs provides abundant chemically active sites for biomolecule conjugation, dispersions of magnetic nanoparticles are attractive in separation applications as they offer high surface area and can be functionalized to selectively discriminate between different molecular or cellular species. A magnet is used to separate the magnetically targeted cells from the non-targeted cells, main advantages of these materials include the low interference, low background signal, no requirement of pre-treatment, and the fact that they can be small enough to be portable.

### **1.3.4 light responsive hydrogel**

Light-sensitive hydrogels have potential applications in developing optical switches, display units, and ophthalmic drug delivery devices. Light-sensitive hydrogels can be

separated into UV-sensitive and visible light-sensitive hydrogels. Unlike UV light, visible light is readily available, inexpensive, safe, clean and easily manipulated. Visible light-sensitive hydrogels were prepared introducing a light sensitive chromophore to poly(N-isopropylacrylamide) hydrogels. When light (e.g.488 nm) is applied to the hydrogel, the chromophore absorbs light which is then dissipated locally as heat by radiationless transitions, increasing the 'local' temperature of the hydrogel. The temperature increase alters the swelling behavior of poly(N-isopropylacrylamide) hydrogels, which are thermo-sensitive hydrogels. The temperature increase is proportional to the light intensity and the chromophore concentration. Light-sensitive hydrogels have potential applications in developing optical switches, display units, and ophthalmic drug delivery devices. Generally, upon the irradiation of light with certain wavelengths, these chromophores reveal changes in their different forms induces macroscopic changes in the structures and thus the properties of the hydrogels, including adhesion, color, permeability, hydrophilicity, ionizability, etc. Base on this, light-responsive hydrogels have been employed to manage size-selective mass transport (electron, gas, inorganic and organic ions) properties, such as color, molecular polarity, molecular size and shape, or transform between ionic state and nonionic state.

### **1.3.5 Electric field responsive hydrogel**

Electric current induced hydrogels are basically composed of polyelectrolyte and shrinks or swells in response to an applied electric field [81]. Polymers contain a large number of the ionizable group on their backbone chain thus sensitive towards both pH and electricity. Electro-sensitive hydrogel, which are basically pH-sensitive hydrogel, are able to convert chemical energy to mechanical energy. Electro-sensitive hydrogel, Electro-sensitive hydrogels undergo shrinking or swelling in the presence of an applied electric field. Sometimes, the hydrogels showswelling on one side and deswelling on the other side. The hydrogel shape change (including swelling, shrinking) depends on a number of conditions. If the surface of hydrogels is in contact with the electrode, the result of applying electric field to the hydrogel may be different from systems where the hydrogel is placed in water (or acetone–water mixture) without touching the electrode. The result will be different yet if the aqueous phase contains electrolytes. Electro-sensitive hydrogels have been applied controlled drug delivery.

## **1.4 Multi responsive hydrogel**

Responsive polymer hydrogels can largely and reversibly change their volume or shapes under slight external stimuli, including temperature, pH, ionic strength, special chemicals, redox, light, humidity, electric field, magnetic fields, etc. This property of responsive polymer hydrogels can be utilized in diverse applications, such as sensor, valve, on-off switches, biomimetic actuators, artificial muscles and so on. A variety of stimuli-responsive hydrogels has been emerging recently, putting this smart hydrogel's responsiveness into use by three dimensional (3D) structure is challenging. Stimuli-responsive polymers are smart polymers which can respond to external stimuli in the form of changing their own properties.

### **1.4.1 Magneto- and thermo-responsive hydrogel**

A specially designed stimuli responsive hydrogel was fabricated. into the network of chemical crosslinked polyacrylamide hydrogel is one of the important environmental factors in typical physiological, biological, chemical systems. AAm hydrogels were aggregated to form physical crosslinks due to the hydrophobic interactions when the pH value of the environment was above 5.0 and the temperature was low. Magnetic nanoparticles incorporate the polymer system but these magnetic nanoparticles are bonded with the polymer system by weak van der Waals force. When the magnetic field applied the magnetic nanoparticle aggregate and break down the weak forces.

### **1.4.2 pH- and Thermo-responsive hydrogel**

pH- and temperature-responsive hydrogels are the most widely investigated intelligent hydrogels because these two stimuli are the most common used external stimuli. This can be a change in conformation, change in solubility, alteration of the hydrophilic/hydrophobic balance or release of a bioactive molecule (e.g. drug molecule). This also includes a combination of several responses at the same time the combination of a pH-responsive system with a thermo-responsive polymer can further alter the hydrophilic/hydrophobic balance. This allows a polymer to become membrane active at a specific temperature and/or a specific pH. Stimuli-responsive hydrogels have recently captured a lot of attention due to their ability to respond to external triggers such as temperature and pH. This makes them attractive candidates for a wide range of biological and biomedical applications.

## **1.5 Magnetic Nanoparticle synthesis method**

### **1.5.1 Thermal decomposition method**

Thermal decomposition Heat is used to cause chemical decomposition of organometallic compounds into monodisperse magnetic nanocrystals. This is achieved in the presence of organic solvents and stabilizing surfactants. Shape and morphology of resulting crystals are mainly controlled through the ratios of the used reagents, reaction temperature and time thermal decomposition complicated as a synthesis technique.

### **1.5.2 Microemulsion method**

As microemulsions are stable dispersions of two liquids, they can be used to synthesize nanoparticles through precipitation caused by the addition of solvents such as ethanol or acetone. The resulting nanoparticle-precipitate can be isolated through centrifugation or filtering. Examples of particulates obtained by microemulsion are gold-coated cobalt/platinum, metallic cobalt and cobalt/platinum alloys.

### **1.5.3 Co-precipitation method**

The most important and established methods of magnetic nanoparticle synthesis are Co-precipitation. A simple and efficient technique to build iron oxides through adding a base to an aqueous  $\text{Fe}^{2+}/\text{Fe}^{3+}$  salt solution at room temperature (or above) and under conditions of inert atmosphere. Co-precipitation very simple, ambient conditions 20 minutes, water needed. As a synthesis technique, co-precipitation is most used, as it is a very efficient and easy. Among various chemical methods for synthesis of different types of metal oxides, co-precipitation method has several advantages over other methods including, good homogeneity, low cost, high purity of product and not requiring organic solvents and heat treatment.

In this research, we aim to synthesize Iron Oxide ( $\text{Fe}_3\text{O}_4$ ) nanomaterials via chemical co-precipitation method combined with nontoxic ferric chloride; ferrous chloride and the toxic sodium hydroxide as starting materials.

## **1.6 Surface modification of Iron oxide nanocomponents**

Bare iron oxide nanoparticles tend to aggregate because of strong magnetic attractions among particles, particle-particle bipolar attraction, the van der Waal force and high

surface energy. On the otherhand when the magnetic nanoparticles are in contact of air, these particles are further oxidized to form alpha or gamma  $\text{Fe}_2\text{O}_3$ . To avoid this problem surface of iron oxide nanoparticles are coated to improve their stability and biocompatibility and to achieve hydrophilicity and conjugating capability. Several coating materials including organic polymers (e.g. dextran, chitosan, polyethylene glycol), organic surfactants (e.g. sodium oleate and dodecylamine), inorganic metals (e.g. gold), inorganic oxides (e.g. silicaoxide and carbon) etc. are used to modify the surface of the magnetic nanoparticles. Here this inorganic oxide such Si act as a stabilizer to prevent aggregation of magnetic iron oxide nanoparticle[8].

### **1.7 Magnetically responsive polymer nanocomponents**

During the last decade, the development of magnetic polymer nanocomponents materials has been the source of discovery of spectacular new phenomena, with potential applications in the multidimensional fields. Among the broad spectrum of nanoscale materials being investigated for various environmental and biomedical applications, magnetic nanoparticles (MNPs) have gained significant attention due to their intrinsic magnetic properties, which makes them successful as magnetically recoverable catalysts, drug delivery agents, anticancer materials, magnetic resonance imaging devices, etc. Magnetic nanoparticles and nanocomposites have aroused significant scientific and technological interest because of their potential applications in the fields of biomedicine, information technology, magnetic resonance imaging, catalysis, telecommunication, and environmental remediation. Magnetic polymer nanocomponents generally comprise of magnetic nanoparticles embedded in polymer matrix. However, magnetic nanoparticles dispersed in composites usually have a strong tendency to form agglomerates for reduction of energy associated with high surface area-to-volume ratio of the nanosized particles. To avoid aggregation of magnetic nanoparticles, protection strategies have been developed to chemically stabilize the magnetic nanoparticle. The properties of magnetic particles remain same after stabilization. So its application in polymer nanocomposites is increasing day by day.

## 1.8 Thermo-responsive polymer nanocomponents

Normally, thermo-responsive hydrogels are prepared from polymers which exhibit – CONH<sub>2</sub> group. To create these surfaces, the temperature-responsive polymer, poly(acrylamide) (PAAm), is bonded with 3D crosslinker by free radical polymerization. As one of the most widely studied smart materials, thermo-responsive hydrogels have attracted an increasing interest and been more and more studied in the past several years, because of the easy controllability of temperature and more importantly their applications in various fields. Critical solution temperature in water, around which the interactions between polymer chains and water vary between hydrophilic state and hydrophobic state dramatically within a small temperature range. Resulting from the expansion or contraction of polymer chains in water, thermo-responsive hydrogels indicate volume phase transition around the lower critical solution temperature (LCST) or upper critical solution temperature (UCST) depending on the polymers. For hydrogels made of polymers with LCST (e.g. poly(N-isopropylacrylamide), PNIPAM), when the temperature lowers below LCST, the gels swell due to the diffusion of water into the polymer networks, because water molecules form hydrogen-bonds with the polar groups on the polymer chains. However, the efficiency of the hydrogen-bonding decreases with the rise in temperature, and when the temperature is above LCST, the hydrophobic property of the polymer chains starts dominating, causing the hydrogels shrink. As a matter of fact, the LCST of thermo-responsive hydrogels can be strongly altered by incorporating certain monomers into the polymer chains. Hydrogels have been properties for their high water content and the possible control over the swelling kinetics make them very attractive for biomedical applications[9].

## 1.9. Swelling properties of hydrogel

A crosslinked polymer hydrogels swell but not dissolve when water or a solvent enters it. The swelling properties, which usually use degree of swelling to define hydrogels, depend on many factors such as network density, solvent nature, polymer solvent interaction parameter. Because of the high water content and biocompatibility of hydrogels, many applications are related to biomedical usage. When a cross-linked polymer keep in a good solvent, it become swell rather than dissolve. Swelling degree define the change of dimension of polymer. A highly cross-linked polymer shows less degree of swelling. The swelling capacity of a polymer is determined by the amount of liquid material that can be



absorbed. The amount of water sorption is quantified by the degree of swelling the ratio of the swollen polymer volume or mass to that of the dry polymer. The swelling value can be calculated by using the following formula ,

$$\text{Swelling \%} = \frac{(W_s - W_d)}{W_d} \times 100\%$$

Where,  $W_d$ = Weight of polymer,  $W_s$ = weight of swollen polymer. The equilibrium swelling degree and the elastic modulus of hydrogels depend on the cross-link and charge densities of the polymer network as well as on the cross-linked polymer concentration after the gel preparation. Polymeric hydrogel networks may be formed by various techniques; however, the most common synthetic route is the free-radical cross-linking copolymerization of a hydrophilic non-ionic monomer such as acrylamide (AAm) with a small amount of 3D cross-linker. In order to increase their gel formation capacity and swelling capacity bi functional crosslinker e.g, N, N'-methylenebis(acrylamide) (MBAAm) is also included into the reaction mixture. Since the monomers for hydrogel preparation are usually solid at the usual polymerization temperature, it is necessary to carry out the polymerization reactions in an aqueous solution. poly(acrylamide) (PAAm) hydrogels prepared from AAm, 3D crosslinker, and MBAAm in aqueous solutions cross-linker concentration dependence of the cross-linking efficiency. MBAAm, that is the fraction of MBAAm forming effective cross-links. Increasing number of ionic groups in hydrogels is known to increase their swelling capacities. This is mainly due to the simultaneous increase of the number of counter-ions inside the gel, which produces an additional osmotic pressure that swells the gel

### 1.10 Literature Review

Stimuli-responsive hydrogels have found increasing attention, which is attributed to the manifold applications they can be used for. Several years intensive research was invested in stimuli-responsive hydrogel. Their stimuli-responsiveness led not only to novel responsive groups, which enabled the translation of an external physical impact into a change of a material property, but also to hydrogel that are equipped with more than one responsive group. The ability of hydrogels to absorb water arises from hydrophilic functional groups attached to the polymer backbone while their resistance to dissolution arises from cross-links between network chains. Water inside the hydrogel allows free diffusion of some solute molecules, while the polymer serves as a matrix to hold water together. Another

aspect of hydrogels is that the gel is a single polymer molecule, that is, the network chains in the gel are connected to each other to form one big molecule on macroscopic scale. Stimuli-responsive hydrogels are cross-linked, hydrophilic polymer networks that undergo a physicochemical transition in response to a change in external stimuli such as pH, temperature, light, ionic strength, electric field, magnetic field and the presence of electrolyte. As a result, dual- or multi-stimuli responsive hydrogel are obtained, which is the starting point to more sophisticated applications, due to the variability that is introduced to the responsiveness. By using this property, it might be used in drug delivery, tissue engineering, biosensors, microfluidic devices, biomedical and application of agricultural field etc. Multi-responsive hydrogel can show more than two stimuli such as pH-, thermo- and light-responsive hydrogel, Light-, Redox- and Temperature-responsive Polymers, Environmental-, pH- and Temperature-responsive hydrogel, Thermo-responsive hydrogel undergoes conformational change in response to temperature change. As designed, the polymer exhibited a responsiveness towards pH, temperature and light and was considered to be triple stimuli- responsive. They show different swelling at different temperature. At a significant temperature range they absorb water and another temperature they squeeze water. Magneto-responsive-hydrogel contain magnetic nanoparticles. This magnetic nanoparticles, dispersed in the polymer system within weak van der Waals force to make the hydrogel magnetically responsive. Applied magnetic field causes the hydrogel to squeeze due to the attraction of the magnetic components to the magnet. At a significant temperature range they absorb water another temperature they squeeze water. By using magnetic property, it may separate from the aqueous solution. This behavior of the magnetic nanoparticles might make things complex when the hydrogel shows regenerability. By using this both property it may use in drug delivery, tissue engineering, and in environmental pollutant remediation. Magnetic nanoparticles are dispersed in the polymer system within Weak Van Der Waals force to make the hydrogel magnetically responsive. When the magnetic field is applied the magnetic nanoparticles aggregate breaking the weak forces and when it is taken off they usually be reluctant to get back to their original position.

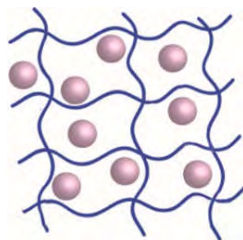


Figure 1.4 magnetic nanoparticles not covalent bonded

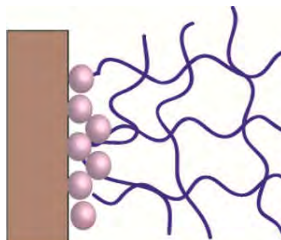


Figure 1.5 Magnetic nanoparticles leave the polymer chain when magnetic field is applied

This is our object. We also synthesized  $\text{Fe}_3\text{O}_4$  and this magnetic nanoparticle also dispersed in the polymer system. But our magnetic nanoparticle dispersed in the polymer system within strong covalent bond. For this when we applied magnetic field the magnetic nanoparticle is not aggregate breaking the strong covalent bond and when the magnetic field is taken off they do not get back their original position.

### 1.11 Research Goal

The interesting behavior of hydrogels has been exploited in a wide variety of applications including drug delivery and tissue engineering, biosensors and microfluidic devices. However, due to the random nature of the crosslinking reactions during the polymerization many polymer gels have poor mechanical properties. This is a significant drawback of the hydrogels restricting their applications specifically where high stress is required [6,7]. Incorporating different materials such as ceramics, metals, silicates and magnetic particles into the hydrogel matrix usually lead to improved properties, enhanced mechanical strength and structural stability. Hydrogel composite systems exploit the individual properties of the components into combined effects increasing the versatility of their applications. Herein, we aim to combine the thermo- and magneto- responsiveness in one hydrogel system and study their properties.

The major goal of this research is to design a noble strategy for the preparation of a magneto- and thermo-responsive nanocomposite hydrogel. Among different external

stimuli for multi-responsive hydrogels, we choose temperature and magnetic field, which are very important in numerous applications including drug delivery and tissue engineering. As thermo-sensitive part of the hydrogel we will use poly(N-isopropylacrylamide), which will be crosslinked with acrylamide-functionalized magnetic nanoparticles to introduce the magnetic responsiveness. The magnetically responsive hydrogels available in the literature are composite of polymer and  $\text{Fe}_3\text{O}_4$  particles where the magnetic  $\text{Fe}_3\text{O}_4$  particles dispersed in the polymer system are held by weak van der Waals force. In our proposed research, the acrylamide-functionalized silica coated  $\text{Fe}_3\text{O}_4$  nanoparticles will be covalently bonded through cross-linking with the polymeric chains of the hydrogel. To achieve our goal first step is to synthesize acrylamide-functionalized silica coated  $\text{Fe}_3\text{O}_4$  that will be used as a general precursor for crosslinking as well as introducing the magnetic properties into the hydrogel. We use this magnetic crosslinker to prepare superabsorbent polyacrylamide hydrogel via in situ polymerization using potassium persulfate as initiator. The as-synthesized nanocomposite will be characterized by x-ray photoelectron spectroscopy (XPS), x-ray diffraction (XRD), scanning electron microscopy (SEM), energy dispersive x-ray (EDX), Fourier transform infrared (FTIR) analyses. Finally, we will investigate the swelling and magnetic behavior of the synthesized superabsorbent nanocomposite hydrogel in water. We expect that this method would be a general platform for the incorporation of magnetic responsiveness through crosslinking of the acrylamide-functionalized magnetic nanoparticles with other polymers like polyacrylamide, polyacrylic acid etc.

## References

1. Chirani, N., Yahia, L.H., Gritsch, L. F., Motta, F.L., Chirani, S., Fare, S., "History and Application of Hydrogel." *Journal of Bio medical science*, vol.4, (2015)
2. Gerlach, G., Arndt, K. F., "Hydrogel Sensors and Actuators." *Springer*, vol.6, (2009)
3. Ahmed E. M., "Hydrogel: Preparation, characterization, and applications: A review." *Journal of Advance Research*, vol. 6(2), pp, 105-121, (2015).
4. Tsitsilianis, C., "Responsive Reversible Hydrogels from Associative "Smart" Macromolecules." *Soft Matter*, vol.6, pp, 2372-2388, (2010).
5. Ge, Z., Hu, J., Huang, F., Liu, S., "Responsive Supramolecular Gels Constructed by Crown Ether Based Molecular Recognition," *Angewandte Chemie International Edition*, vol.48, pp 1798-1802, (2009).
6. Chen, G., Hoffman, A.S., "Graft Copolymers that Exhibit Temperature-Induced Phase Transitions Over a Wide Range of pH," *Nature*, vol.373, pp, 49-52 (1995).
7. Ghosh, R., Mah, E., "Thermo-Responsive Hydrogels for Stimuli-Responsive Membranes." *Processes*, vol.1(3), pp, 238-262, (2013).
8. Wu, W., He, Q., and Jiang, C., "Magnetic Iron Oxide Nanoparticles: Synthesis and Surface Functionalization Strategies." *Nanoscale*, vol.3(11), pp, 397-415, (2008)
9. Ward, M. A., Georgiou, T.K., "Thermo-responsive Polymers for Biomedical Applications." *Polymers*, vol.3, pp, 1215-1242, (2011).
10. Pochan, D. J., Schneider, J. P., Kretsinger, J., Ozbas, B., Rajagopal, K., Haines, L., "Thermally Reversible Hydrogels via Intramolecular Folding and Consequent Self-Assembly of a De Novo Designed Peptide," *Journal of American. Chemical Society*, vol. 125(39), pp 11802-11803, (2003)
11. Banet, P., Griesmar, P., Serfaty, S., Vidal, F., Jaouen, V., Huerou, Y.L., "One – Shot Synthesis of a Poly (N-isopropylacrylamide)/Silica Hybrid Gel," *Journal of Physical Chemistry*, vol. 113(45), pp. 14914-14919, (2009).
12. Xiao, Y., He, L., Che, J., "An Effective Approach for the Fabrication of Reinforced Composite Hydrogel Engineered with SWNTs, Polypyrrole and PEGDA Hydrogel," *Journal of Materials Chemistry*, vol. 22, pp, 8076-8082 (2012)
13. Hsu, L., Weder, C., Rowan, S. J., "Stimuli-responsive, Mechanically-Adaptive Polymer Nanocomposites," *Journal of Materials Chemistry*, vol. 21, pp. 2812-2822, (2011).

14. Peng, J., Liu, Q., Xu, Z., Masliyah, J., “Synthesis of Interfacially Active and Magnetically Responsive Nanoparticles for Multiphase Separation Application”, *Journal of Advanced Functional Materials*, vol. 22, pp. 1732-1740, (2012).
15. Azam, M. S., Fenwick, S. L., Gibbs-Davis J.M., “Orthogonally Reactive SAMs as a General Platform for Bifunctional Silica Surface,” *Langmuir*, vol. 27(2), pp. 741-750 (2011).
16. Xu, J., Ju, C., Sheng, J. Wang, F., Zhang, Q., Sun, G., Sun, M., “Synthesis and characterization of magnetic nanoparticles and its application in lipase immobilization”, *Bull. Korean Chem. Soc.*, vol. 34(8), pp 2409-2412,(2013).
17. Yan, W., Bin, H., Xiaoyang,H.,Yuanhua, L.,Xinzhi, W., Xuliang, D., “Synthesis of Fe<sub>3</sub>O<sub>4</sub> nanoparticles and their magnetic properties.” *Procedia Engineering* vol. 27. pp 632-637 (2012).
18. Camargo, P. H. C., Satyanarayana, K. G., Wypych, F., “Nanocomposites: Synthesis, Structure, Properties and New Application Opportunities.” *Materials Research*, vol. 12(1), pp. 1-39, (2009).
19. Zhu, J., Wei, S., Chen, M., Gu, H., Rapole, S. B.; Pallavkar, S.; C. Ho, T.; Hopper, J.; Guo, Z.; “Magnetic nanocomposites for environmental remediation”, *Advanced Powder Technology*, vol. 24, pp. 459–467, (2013).
20. Jafarbeglou, M., Abdouss, M., Shoushtari, A. M., Jafarbeglou, M., “Clay nanocomposites as engineered drug delivery systems”, *RSC Adv.*, vol.6, pp. 50002-50016, (2016).
21. Iliescu,R. I., Andronescu,E., Ghitulica,C. D., Voicu, G., Fikai, A., Hoteteu, M., “Montmorillonite–alginate nanocomposite as a drug delivery system – incorporation and in vitro release of irinotecan”, *International journal of Pharmaceuticals* 2014,vol. 463,pp. 184–192, (2014).
22. Jones, W. E., Chiguma, J., Johnson, E., Pachamuthu, A., Santos, D., “Electrically and Thermally Conducting Nanocomposites for Electronic Applications”, *Materials*, vol. 3, pp. 1478-1496, (2010).
23. Snezana, I.,Nikoli, L., Nikoli, V., Petrovi, S., Stankovi, M., “Stimuli-sensitive hydrogels for pharmaceutical and medical application.” vol. 9, No1, 2011, pp. 37 – 56 , (2011).

24. Chirta, M., Grozescu, I., “Fe<sub>2</sub>O<sub>3</sub> – Nanoparticles, Physical Properties and Their Photochemical and Photo electro chemical Applications” *Politehnica*, vol. 54(68), p 1, (2009).
25. Medeiros, S. F., Santos, A.M., Fessi, H., Elaissari, A., “Stimuli-responsive magnetic particles for biomedical applications.” *International Journal of Pharmaceutics*, vol.403, pp. 139–161, (2011).
26. Lin, X., Quoc, B. N., Ulbricht, M., “Magneto-responsive polyethersulfone-based iron oxide cumhydrogel mixed matrix composite membranes for switchable molecular sieving.” *Applied Materials & Interfaces* vol. 8 (42), pp 29001–29014, (2016).
27. Yoshida, R., Okano, T. “Stimuli-Responsive hydrogel and their application to Functional Materials.” *Biomedical Applications of Hydrogels Handbook*, pp.19-43, (2013).
28. Krogsgaard, M., Behrens M.A., Pedersen, J.S., and Birkedal, H., “Self-Healing Mussel-Inspired Multi-pH-Responsive Hydrogels.” *Biomacromolecules* 2013, vol. 14, pp. 297–301, (2013).
29. Gong, X. L., Xiao, Y. Y., Pan, M., Kang, Y., Li, B.J., Zhang, S., “pH- and Thermal-Responsive Multi-Shape Memory Hydrogel.” *Applied Materials & Interfaces*. vol.8 (41), pp. 27432–27437, (2016).
30. Dave, P. N., Chopda, L.V., “Application of Iron Oxide Nanomaterials for the Removal of Heavy Metals.” *Journal of Nanotechnology* vol. 2014, Article ID 398569, 14 pages, (2014).
31. Yang, X., Ma, C., Li, C., Xie, Y., Huang, X., Jin, Y., Zhu, Z., Liu, J., Li, T., “Three Dimensional Responsive Structure of Tough Hydrogels.” *Electroactive Polymer Actuators and Devices*, vol. 9430, pp. 94301F-1-F5, (2015).
32. Ward, M.A., Georgiou, T.K., “Thermo-responsive Polymers for Biomedical Applications.” *Polymers*, vol.3, pp. 1215-1242, (2011).
33. Syed, B. K., Gulrez, H., Assaf, S.A., and Phillips, G. O., “Hydrogels: Methods of Preparation, Characterization and Applications.” Book. Chapter 5 pp. 117-150
34. Ahmed, E.M., “Hydrogel: Preparation, characterization, and applications: A review.” *Journal of Adv. Research*. vol.6(2), pp. 105–121, (2015).
35. Ullah, F., Bisyrul, M., Othman, H., Javed, F., Ahmed, Z., Akil H.M., “Classification, Processing and Application of Hydrogels: A Review.” *Materials science and Engineering*, vol.57, pp. 414-433, (2015).

36. Calo, E., khutoryanskiy, V.V., "Biomedical applications of hydrogels: A review of patents and commercial products." *European polymer Journal*, vol.65, pp. 252-267, (2015).
37. Ionov, L., "Hydrogel-based actuators: possibilities and limitations." *Journal Materials* vol.17(10) pp. 494-503, (2014).
38. Nicoletta, F. P., Cupelli, D., Formoso, P., Filpo, G. D., Colella, V., and Gugliuzza, A., "Light Responsive Polymer Membranes: A Review." *Journal of Membranes*, vol. 2, pp. 134-197, (2012).
39. Sahoo, S.K., De, T.K., Ghosh, P.K., Maitra, A., "pH- and Thermo-Sensitive Hydrogel Nanoparticles." *Journal of Colloid and Interface Science*, vol.206(2) pp. 361-368, (1998).
40. Fundueanu, G., Constantin, M., Bucatria, S., Ascenzi, P., "pH/thermo-responsive poly(*N*-isopropylacrylamide-*co*-maleic acid) hydrogel with a sensor and an actuator for biomedical applications" *Journal of Polymer*, vol. 110, pp. 177–186, (2017).
41. Constantin, M., Bucatariu, S., Harabagiu, V., Popescu, I., Ascenzi, P., Fundueanu, G. "Poly(*N*-isopropyl acrylamide-*co*-methacrylic acid) pH/thermo-responsive porous hydrogels as self-regulated drug delivery system." *Journal of Pharmaceutical Science*, vol.62, pp 86-95, (2014).
42. Wu, W., He, Q., and Jiang C., "Magnetic Iron Oxide Nanoparticles: Synthesis and Surface Functionalization Strategies." *Nanoscale*, vol.3 (11) pp. 397-415, (2008).
43. Wu, W., Jiang, C.Z., and Roy, V.A.L., "Designed synthesis and surface engineering strategies of magnetic iron oxide nanoparticles for biomedical applications." *Journal of Nanoscale*, I.47, pp. 421-474, (2016).
44. Roberts, A. P., Liu, Q., Rowan, C. J., Chang, L., Carvalho, C., Torrent, J., and Horng, J. S., "Characterization of hematite ( $\alpha$ -Fe<sub>2</sub>O<sub>3</sub>), goethite ( $\alpha$ -FeOOH), greigite (Fe<sub>3</sub>S<sub>4</sub>), and pyrrhotite (Fe<sub>7</sub>S<sub>8</sub>) using first-order reversal curve diagrams." *Journal of Geophysics*. vol.111, pp. B12-S35, (2006).
45. Blanney, L., "Magnetite (Fe<sub>3</sub>O<sub>4</sub>): Properties, Synthesis, and Applications" vol. 15 pp. 33-78, (2007).
46. Akbarzadeh, A., Samiei, M., and Davaran, S., "Magnetic nanoparticles: preparation, physical properties, and applications in biomedicine." *Journal of Nanoscale*, vol.7(1), p. 144, (2012).



47. Ramesan, M. T., “Effects of magnetite nanoparticles on morphology, processability, diffusion and transport behavior of ethylene vinyl acetate nanocomposites.” *International Journal of Plastic and Technology* vol.19(2) pp. 368-380, (2015).
48. Zou, H.; Wu, S.; Shen, J.; “Polymer/Silica Nanocomposites: Preparation, Characterization, Properties, and Applications”, *Chem. Rev.*, vol. 108, pp. 3893–3957,(2008).
49. He, J.; Shen, Y.; Yang, J.; Evans, D. G.; Duan, X.; “Nanocomposite structure based on silylated mcm-48 and poly(vinyl acetate)”, *Chem. Mater.*, vol.15, pp. 3894-3902, (2008).
50. Ciprari, D.; Jacob, K.; Tannenbaum, R.; “Characterization of polymer nanocomposite interphase and its impact on mechanical properties”, *Macromolecules*, vol. 39, pp. 6565-6573, (2006).
51. Zhou, C.; Wu, Q.; “A novel polyacrylamide nanocomposite hydrogel reinforced with natural chitosan nanofibers”, *Colloids and Surfaces B: Biointerfaces*, vol. 84, 155–162, (2011).
52. Zhu, J., Wei, S., Chen, M., Gu, H., Rapole, S. B., Pallavkar, S., C. Ho, T., Hopper, J., Guo, Z., “Magnetic nanocomposites for environmental remediation”, *Advanced Powder Technology*, vol. 24, 459–467, (2013).
53. Camargo, P. H. C.; Satyanarayana, K. G.; Wypych, F. Nanocomposites: Synthesis, Structure, Properties and New Application Opportunities, *Materials Research*, vol. 12(1), pp. 1-39, (2009).

# **Chapter 2**

# **Experimental**

## 2.1 Materials and Instrument

### 2.1.1 Chemicals and Reagents

In this research, we used most of the chemicals of Merck, Germany and Sigma Aldrich. Some chemicals are of BDH. The chemicals and reagents used in this work were analytical grade. They were used without further purification. Distilled water was used as solvent to prepare most of the solutions of this work.

### 2.1.2 Materials

The chemicals and reagents which are used in this research are given below:

- i. Ethanol (Merck, Germany)
- ii. Toluene (Merck, Germany)
- iii. Sodium hydroxide (Merck, Germany)
- iv. Potassium per sulfate (BDH)
- v. Sulfuric acid (Merck, Germany)
- vi. Hydrochloric acid (analytical grade)
- vii. Acetone (analytical grade)
- viii. Ferrous chloride.  $4\text{H}_2\text{O}$ (Sigma Aldrich)
- ix. Ferric chloride.  $6\text{H}_2\text{O}$ (Sigma Aldrich)
- x. Ammonia solution (25%)
- xi. Tetraethyl orthosilicate (TEOS) (Sigma Aldrich)
- xii.  $\gamma$ -aminopropyl triethoxy silane (APTES) (Sigma Aldrich)
- xiii. N,N'-diethylformamide (DMF) (Merck, Germany)
- xiv. Methacrylic anhydride (Sigma Aldrich)
- xv. Acrylamide (BDH)
- xvi. N,N'-methelynebisacrylamide (Sigma Aldrich)
- xvii. Hydrogen peroxide (Org Germany)

### 2.1.3 Instruments

Analysis of the samples was performed using the following instruments:

- i. Fourier Transform Infrared Spectrophotometer (SHIMADZU FTIR-8400)
- ii. Field Emission Scanning Electron Microscopy (JSM-7600F, Tokyo, Japan)
- iii. X-ray Diffractometer (Philips, Expert Pro, Holland)
- iv. X-ray photoelectron Spectroscopy
- v. Centrifuge machine (Hettich, Universal 16A)
- vi. pH meter (Hanna, HI 8424, Romania)
- vii. Digital Balance (AB 265/S/SACT METTLER, Toletto, Switzerland)
- viii. Freeze dryer (Heto FD3)

## 2.2 Synthesis of magnetic crosslinker

### 2.2.1 Synthesis of Fe<sub>3</sub>O<sub>4</sub>

The magnetite (Fe<sub>3</sub>O<sub>4</sub>) nanocomponents prepared by the most popular, easy and widely used, chemical co-precipitation method. An iron salt solution was obtained by mixing 0.005mol 2.70g FeCl<sub>3</sub> and 0.0025mol 0.633g FeCl<sub>2</sub> such that the ratio of Fe<sup>3+</sup> to Fe<sup>2+</sup> in 50ml deoxygenated distilled water by passing N<sub>2</sub> gas about 10 min. Twenty milliliter of 1.5M NaOH was rapidly poured into the ferric salt solution under magnetic stirring at room temperature (RT). Orange color of iron salt solution was instantly changed and black precipitate found. After continuously stirring for 20min, the precipitate was separated by magnetically and washed with the deoxygenated distilled water four times by centrifugation. Obtained this sample called S1. And take some sample for FTIR and oven dried at 50°C overnight. the naked Fe<sub>3</sub>O<sub>4</sub> nanocrystals were obtained as the control sample (called S1).

### 2.2.2 Silica coated Fe<sub>3</sub>O<sub>4</sub>

Magnetic Fe<sub>3</sub>O<sub>4</sub> nanocrystals were coated by hydrolysis of TEOS on the surfaces of the magnetic Fe<sub>3</sub>O<sub>4</sub> nanocrystals in basic solution via stobers method. After washing with the anhydrous ethanol, the precipitate Fe<sub>3</sub>O<sub>4</sub> was ultrasonically dispersed in a solution

containing 240ml ethanol and 60ml water, then loaded into a three-necked bottle. The pH value was adjusted to 9 with 25% ammonia solution. Here 300 mg magnetic nanoparticle were dispersed in the solution. Add 4ml TEOS under vigorous stirring. The resulting dispersion was mechanically stirred for 10 hours. After 10h, the ferrofluid was heated at 50°C to complete hydrolysis for another 12h, and a little was removed to prepare a SEM sample. The particles were again separated by centrifugation and washed with the deoxygenated distilled water and anhydrous ethanol, then vacuum-dried at 50°C overnight. The silica-coated Fe<sub>3</sub>O<sub>4</sub> nanocrystals were prepared and the sample was called S2.

### **2.2.3 Silica coated Fe<sub>3</sub>O<sub>4</sub> functionalized by –NH<sub>2</sub> group**

After washing with the anhydrous ethanol in step 2, then washed with dimethyl formamide (DMF). Then the silica-coated Fe<sub>3</sub>O<sub>4</sub> nanocrystals were ultrasonically dispersed in a solution containing 120ml DMF and 80ml toluene, then loaded into a three-necked bottle as above. Ten milliliter 10mL (3-aminopropyltriethoxysilane) APTES was added drop by drop into the three necked bottle under magnetic stirring. After hydrolyzing for 24hour at room temperature, the particles were collected by centrifugation and washed within toluene 4 times. The silica-coated Fe<sub>3</sub>O<sub>4</sub> nanocrystals functionalized by –NH<sub>2</sub> groups were thus obtained and were called S3[10].

### **2.2.4 Further functionalized by –CH=CH<sub>2</sub> group**

After washing with toluene for the last time in step 3, the particles were redispersed in 150 ml toluene and loaded into a three-necked bottle and heated at 120°C until half of the solution became 90 ml, so that the water was thoroughly removed. After reaching that volume heating stopped and kept for cool down at room temperature. Always covered the flask tightly because water absorbed by the sample. After that 6.7mL methacrylic anhydride was added to the sample and magnetically stirred about 4 hours. Finally, the sample was washed with toluene several times and kept in toluene and got acrylic modified magnetic iron oxide nanoparticles. It is very essential to keep the sample into water for future reaction. For this solvent exchange needed from toluene to water. Toluene and water are practically insoluble in each other. Toluene and acetone are miscible in all proportions, as are also acetone and water. For this reasons acetone was added to sample in toluene and after that solvent was removed. This was repeated several times and as a result toluene was almost completely removed. After that, water was added to the sample

in acetone. This was repeated several times and the sample was heated at 58<sup>0</sup>C. As a result, acetone was removed and the sample retained in water. We were thus obtained, and this sample was called S4.

### **2.3 Synthesis of nanocomposite**

PAAm / Fe<sub>3</sub>O<sub>4</sub> nanocomposite was synthesized via in situ process. Firstly, sonicate S4 sample for 10 min. Take 1.25 mL acrylated MION that contain 6.25 mg magnetic crosslinker into a vial and another vial 10 mg of potassium per sulfate (KPS) dissolve with 2 ml distill water and mixed it. After that this sample sonicate 5 min under 30<sup>0</sup>C temperature. Take 2g acrylamide with 4ml distill water into a testube and add 1 mg N, N'-methylene bis acrylamide (MBA) with 2ml distill water on a hot plate and set temperature 65<sup>0</sup>C. Then add dropwise the sample acrylated MION and KPS into the test tube. Here we maintain total volume of 10 mL. Finally, free radical polymerization was allowed to continue by adding KPS solution dropwise. This mixture was heated at 65<sup>0</sup>C and continuously stirring at 1200 rpm for 4 hours [2,3]. After completion of the reaction, resulting nanocomposite was dried with vacuum oven. After dried this sample collect. we also synthesize that contain 3.125 mg Acrylated MION and without acrylated MION follow this procedure and also maintain total volume of 10 mL. To get such type of nanocomposite we synthesized nanocomposite varying the amount of Acrylamide, magnetic crosslinker. The varied ratio of Acrylamide, and magnetic crosslinker is 2:0, 2:0.00625, 2:0.00312. We also follow this ratio 4:0 g, 4:0.025 g, 4:0.05 g. For the synthesis of nanocomposite, we also synthesize without N, N'-methylenebisacrylamide,(MBA)to see the crosslinker effect.

### **2.4 Swelling study of hydrogel**

#### **2.4.1 Kinetics study of swelling**

The dried hydrogels were left to swell in distilled water at room temperature for different time interval. Firstly, cut the sample small pieces that contain 0.1g or around 0.12 g. Take the three sample into three 100mL beaker and add distill water. After 0.5 hour we keep the sample on a Petri disk and weight the sample by the digital balance and measure the swelling ratio. Follow this process fixed time interval that 1h, 2h, 4h, 8h, 16h, 32h, measure the swelling ratio. Swollen gels were removed from swelling medium at regular interval of

time and dried superficially with filter paper, weight and placed in the same medium. The measurements were continued until a constant weight was reached for each sample.

#### **2.4.2 Temperature dependent swelling study**

Three sample (4:0.0125g, 4:0.025g, 4:0.0g) cut around 0.12 g and take the sample into three 100 mL beaker and put this beaker on a water bath at 30<sup>0</sup>C for 48 h. Sometimes check the temperature. After 48 h weighted the sample and measure the swelling ratio and also measure the swelling percentage. Follow this procedure we measured the swelling ratio at 34<sup>0</sup>C, 38<sup>0</sup>C, 42<sup>0</sup>C. Only one sample was carried out two temperatures.

#### **2.5 Self-healing analysis**

The self-healing experiments were carried out following our previously reported. A ~1.0 cm diameter hole was artificially punched in the middle of a ~2.0 cm diameter long hydrogel disk, and then photos were taken at different time intervals to monitor the self-healing process. Self-healing hydrogels are considered to be injectable materials because of their automatic self-repair capability after damage, similar to some biological systems. Our hydrogel contains magnetic crosslinker that have Fe<sub>3</sub>O<sub>4</sub> but less amount than literature. The Fe<sub>3</sub>O<sub>4</sub>/PAM hydrogel had self-healing ability in the ambient environment without any other external stimuli that was ascribed to strong covalent bond.

#### **2.6 Fourier transform infrared analysis (FTIR)**

The infrared spectra of the polymer nanocomposite, c magnetic iron oxide nanoparticle, silica coated magnetic iron oxide, aminated magnetic iron oxide (silica coated iron oxide), acrylated magnetic iron oxide nanoparticle, polymer nanocomposite, sample recorded on an FTIR spectrometer in the region of 4000 – 400 cm<sup>-1</sup>. For FTIR every step we keep some sample into vial and oven dried under 50<sup>0</sup>C. A small portion of dried sample grinded as much as possible. On the otherhand silica coated magnetic iron oxide nanoparticles, aminated magnetic iron oxide (silica coated magnetic iron oxide nanoparticles), acrylic modified magnetic iron oxide nanoparticles were dried and grinded into a mortar with a pestle. After synthesis polymer nanocomposite we cut the gel as small size and put into the vial for dried here only use freeze dryer. After dryer it also grinded as much as possible. The powder mixture was then compressed in a metal holder under a pressure of

8–10 tons to make a pellet. The pellet was then placed in the path of IR beam for measurements.

### **2.7 Field emission scanning electron microscopy (SEM)**

The surface morphology of the synthesized magnetic iron oxide nanoparticles, silica coated MION, amino propyl(silica coated magnetic iron oxide nanoparticles), acrylic modified magnetic iron oxide nanoparticles, PAA/Fe<sub>3</sub>O<sub>4</sub> nanocomposite was adopted using Field Emission Scanning Electron Microscopy (FE-SEM). For SEM sample preparation we use glass slide. For clean and removing organic substrate use piranha solution in 2 : 1 molar of sulfuric acid(H<sub>2</sub>SO<sub>4</sub>) and Hydrogen peroxide(H<sub>2</sub>O<sub>2</sub>) After drying the glass slide we put 1 or 2 drop from the more and more diluted sample. The completely freeze dried samples were glued on a conducting carbon strip. The sample loaded strip was then mounted to a chamber that evacuated to  $\sim 10^{-3}$  to  $10^{-4}$  tor and then a very thin platinum layer (few nanometers thick) were sputtered on the sample to ensure the conductivity of the sample surface. The sample was then placed in the main FESEM chamber to view its surface. The microscope was operated at an accelerating voltage of 5.0 kV. The system was computer interfaced and thus provides recording of the surface images in the computer file for its use as hard copy.

### **2.8 Energy dispersive x-ray (EDX) spectroscopy**

Elemental analysis of the synthesized magnetic iron oxide nanoparticles(MION),silica coated MION, acrylic modified magnetic iron oxide nanoparticles, PAAm/Fe<sub>3</sub>O<sub>4</sub> nanocomposite were performed by EDX spectra. The glass slide that contain these sample were placed on a 1 cm × 1cm conducting steel plate. The steel plate was then placed on a conducting carbon glued strip. The sample was then placed in the main FESEM chamber integrated.

### **2.9 X-ray diffraction (XRD)**

Magnetic iron oxide nanoparticles, modified Fe<sub>3</sub>O<sub>4</sub> were analyzed for their X-ray diffraction pattern in the powder state. The powder samples were pressed in a square aluminum sample holder (40mm × 40mm) with a 1 mm deep rectangular hole (20mm × 15mm) and pressed against an optical smooth glass plate. The upper surface of the sample



was labeled in the plane with its sample holder. The sample holder was then placed in the diffractometer.

### **2.10 X-ray photoelectron spectroscopy (XPS)**

XPS measurements were performed on samples that had been prepared within 4 days using the AXIS ULTRA spectrometer (Kratos Analytical). The base pressure in the analytical chamber was  $<3 \times 10^{-8}$  Pa. The monochromatic AlK $\alpha$  source ( $h\nu=1486.6\text{eV}$ ) was used at a power of 210 W. The photoelectron exit angle was  $90^\circ$ , and the incident angle was  $35.3^\circ$  from the plane of the surface. The analysis spot was  $400 \times 700\mu\text{m}$ . Survey scans were collected for binding energies from 1100 to 0eV with analyzer pass energy of 160eV and a step of 0.35eV. The high-resolution spectra were run with a pass-energy of 20eV and a step of 0.1eV. Relative sensitivity factors (RSFs) for different elements were as follows: 1 for C (1s), 1.8 for N (1s), 2.93 for O (1s), 0.26 for Si (2s), 0.27 for Si (2p). Only one set of XPS scans was performed on a given sample; therefore, XPS analysis before and after surface reactions were performed on different samples.

## References

1. He, Y. P., Wang, S.Q., Li, C.R., Miao, Y.M., Wu, Z. Y., Zou, B.S., “Synthesis and characterization of functionalized silica-coated Fe<sub>3</sub>O<sub>4</sub> superparamagnetic nanocrystal for biological applications.” *Journal of Physics D: Applied Physics*, vol. 38, pp. 1342–1350 (2005).
2. Zhou, L., He, B., and Huang, J., “One-Step of Robust Amine-and Vinyl-Capped Magnetic Iron Oxide Nanoparticles for Polymer Grafting, Dye Adsorption, and Catalysis.” *Journal Applied Materials and Interfaces*, vol.5, pp. 8678-8685, (2013).
3. Ghazanfari, M. R., Kashefi, M., Shams, S. F., and M. R. Jaafar, M. R., “Perspective of Fe<sub>3</sub>O<sub>4</sub> Nanoparticles Role in Biomedical Applications.” *Biochemistry Research International*. Vol. 32 p. 32 (2016).
4. Wu, W., He, Q., and C. Jiang, C., “Magnetic Iron Oxide Nanoparticles: Synthesis and Surface Functionalization Strategies.” *Journal of nanoscale* vol.3(11). pp. 397-415, (2008).
5. Ganji, F., Farahani, S. V., and Farahani, E. V., “Theoretical Description of Hydrogel Swelling: A Review.” *Iranian Polymer Journal*, vol. 19(5), pp. 375-398, (2010).
6. Gupta, N. V., Shivakuma, H. G., “Investigation of Swelling Behavior and Mechanical Properties of a pH-Sensitive Super Porous Hydrogel Composite.” *Iranian Journal of Pharmaceutical Research*, vol.11(2), pp. 481-493, (2012).
7. Koç, M.L., Ozdemir, U., Imren, D., “Prediction of the pH and the temperature-dependent swelling behavior of Ca<sup>2+</sup>-alginate hydrogels by artificial neural networks.” *Chemical Engineering Science*, vol. 63pp. 2913—2919, (2008).

# **Chapter 3**

## **Results and Discussion**

### 3.1 Synthesis of magnetic nanocomposite

#### 3.1.1 Synthesis of magnetic crosslinker

Crosslinker plays a vital role for linking one polymer chain to another polymer chain. There are three types of crosslinker. These are 1D crosslinker, 2D crosslinker, 3D crosslinker. Among these crosslinkers are commercially available and some are lab prepared. Among different crosslinkers 3D crosslinker has comparatively larger surface area and reactive sites than conventional linear or planar crosslinker. In our study we developed a magnetic 3D crosslinker. For magnetic property magnetic iron oxide nanoparticles (MION) were synthesized via co-precipitation method. Where we used 2:1 molar ratio of  $\text{Fe}^{2+}$  and  $\text{Fe}^{3+}$  salt and 1.5 M NaOH solution. During this reaction we deoxygenated water by passing  $\text{N}_2$  gas so that produced magnetic iron oxide nanoparticles could not come in contact with  $\text{O}_2$ . If these nanoparticles come in contact with air, it oxidized to  $\text{Fe}_2\text{O}_3$ . For these reason coating of nanoparticles is very essential and this urgent work was done by coating with silica using tetraethylorthosilicate (TEOS) in basic medium (25%  $\text{NH}_3$  solution). This was done in two steps. First step, after addition of TEOS stirred 10h without heat. Next step was carried out applying heat at  $50^\circ\text{C}$  for 12h so that completely coated with silica. Here act as a stabilizer, prevent magnetic particle-particle bipolar interaction. Now our target is to add such group which would link up with polymer chain. For this purposes silica coated MION was functionalized with amino group followed by treated with APTES (3-aminopropyltriethoxysilane). In addition to the  $-\text{OH}$  groups on the surface can easily covalent with  $-\text{NH}_2$  group. Finally treated with methacrylic anhydride and found acrylic group at the end of the chain. This acrylic group is able to link polymer chain and acrylated MION act as magnetic crosslinker.

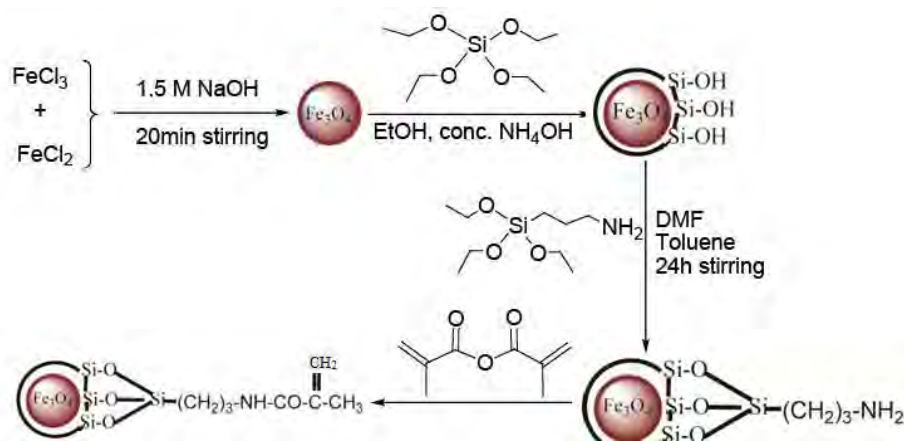


Figure: 3.1 Schematic representation of magnetic crosslinker

### **3.1.2 Polymer nanocomposite Synthesis**

For the synthesis of nanocomposite, magnetic crosslinker were sonicated 10 min so that the aggregated particles apart from each other. After that 2g acrylamide, 1 mg N,N'-methylenebisacrylamide, (MBA) dissolve and mixed with each other into the test tube. Again magnetic crosslinker with KPS sonicate 5 minutes and this case temperature kept below 30<sup>0</sup>C. After that this solution add dropwise into the test tube and this case temperature was 65<sup>0</sup>C. During sonication dissolved potassium per sulfate (KPS) which is as initiator added rapidly. After the addition of initiator KPS and magnetic crosslinker the polymerization start. As we use magnetic crosslinker which has manifold reactive sites hence many more polymer chains linked by the crosslinker. We use this magnetic crosslinker to prepare superabsorbent polyacrylamide hydrogel via in situ polymerization using potassium per sulfate as initiator.

Our target is to make such a nanocomposite which act as multi responsive that magneto- and thermo- responsive nanocomposite. For these highly reactive sites of magnetic crosslinker are able to link with many polymer chains that contain magnetic nanoparticle. For thermo- responsiveness we use acrylamide.

### **3.2 Functional group analysis using FTIR**

the FTIR spectra of magnetic iron oxide nanoparticles (MION) and modified MION. The 1<sup>st</sup> one is for MION. The strong absorption peak at 578 cm<sup>-1</sup> attribute to the vibration of Fe-O bond and this is the characteristic peak of naked Fe<sub>3</sub>O<sub>4</sub>. This also indicates the resonance with oxygen. The peak at 1627 cm<sup>-1</sup> indicates the presence of O-H vibration in H<sub>2</sub>O and the peak at 3425 cm<sup>-1</sup> is attributed to the stretching vibrations of OH adsorbed on the surface of the Fe<sub>3</sub>O<sub>4</sub> nanoparticle. The 2<sup>nd</sup> one is for silica coated iron oxide nanoparticle. The strong peaks at 1080 cm<sup>-1</sup> and 804 cm<sup>-1</sup> have been assigned to the asymmetric and symmetric linear stretching vibrations of Si-O-Si bonding. The bending vibration absorption peaks of Si-O-Si and Si-OH were observed at 461 cm<sup>-1</sup> and 962 cm<sup>-1</sup> respectively. These indicates that the successfully coating of silica layer another surface of magnetic iron oxide nanoparticles.

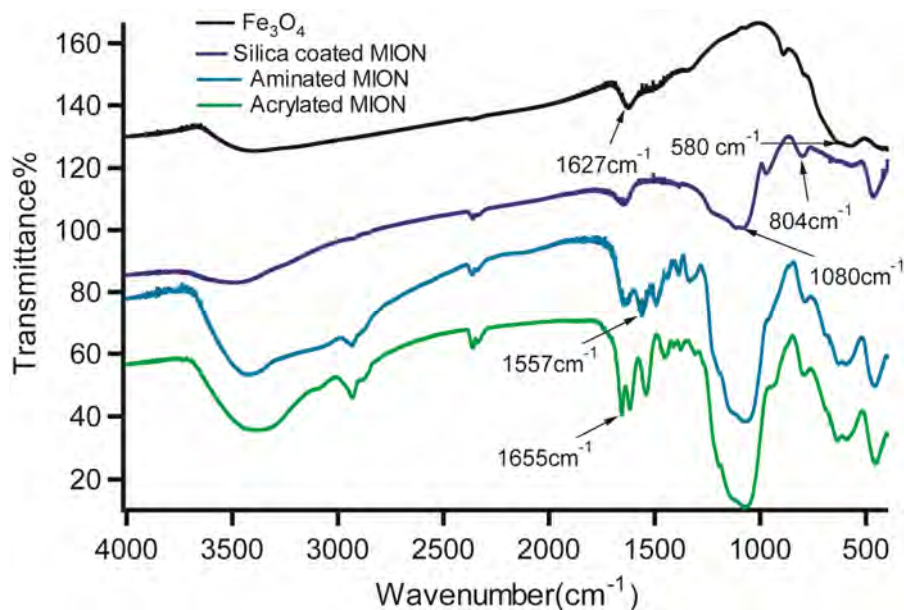


Figure 3.2 FTIR spectra of Fe<sub>3</sub>O<sub>4</sub>, silica coated MION, aminated MION and acrylated MION

In the spectrum of aminated MION, the two bands at 3422 cm<sup>-1</sup> and 1650 cm<sup>-1</sup> can be referred to the N-H stretching vibration and NH<sub>2</sub> bending mode of free NH<sub>2</sub> group, respectively [5]. The antisymmetric C-H stretching vibrations appeared at 2935 cm<sup>-1</sup>, and the bending vibration absorption peaks of -CH<sub>2</sub> and -CH<sub>3</sub> appeared in 1492 cm<sup>-1</sup> and 1385 cm<sup>-1</sup>, respectively; The C-N stretching vibrations appeared at 1335 cm<sup>-1</sup>. The deformation vibration absorption peak of N-H appeared at 1553 cm<sup>-1</sup>. These indicate the successful introduction of APTES to the surface of silica coated magnetic NPs. The 4<sup>th</sup> one is for acrylated MION. The sharp peak at 1655 cm<sup>-1</sup> is the characteristic peak of C=C bond. From this we confirm that acrylic group is successfully added. All characteristic peaks of MION, Silica coated MION, Aminated MION, Acrylated MION that are found in our study are shown in table 3.1.

Table 3.1 Characteristic IR band of MION, Silica coated MION, Aminated MION, Acrylated MION

Wavenumber (cm <sup>-1</sup> )	Interpretation
580	Fe-O vibration
1627	O-H vibration in H <sub>2</sub> O
3425	O-H stretching vibration in H <sub>2</sub> O

804	Si-O-Si Symmetric stretching vibration
1080	Si-O-Si Asymmetric stretching vibration
962	Si-OH bending vibration
3422	N-H stretching vibration
1650	NH <sub>2</sub> bending vibration
2935	C-H Anti symmetric stretching vibration
1492	-CH <sub>2</sub> bending vibration
1385	-CH <sub>3</sub> bending vibration
1335	C-N stretching vibration
1557	N-H vibration
1655	C=C vibration

From the nanocomposite FTIR spectra absorption peak at 3435.84 cm<sup>-1</sup>, attributed to the -NH<sub>2</sub> stretching vibrations of the polyacrylamide nanocomposite. A broad band in the range of 2860 - 2930 cm<sup>-1</sup> was also assigned to the characteristic absorption peak of the symmetric and asymmetric stretching vibration of -CH<sub>2</sub> group and the band at 1631 cm<sup>-1</sup> was distributed to the stretching vibration of -C=O in polyacrylamide nanocomposite. It was observed that, the IR spectra of all samples clearly reveal the presence of strong IR absorption bands at between 400 and 700 cm<sup>-1</sup>, which are the characteristic absorption peaks of Fe-O vibration related to Fe<sub>3</sub>O<sub>4</sub>. Respectively indicate 1668 and 1720 cm<sup>-1</sup> amide and carboxyl groups.

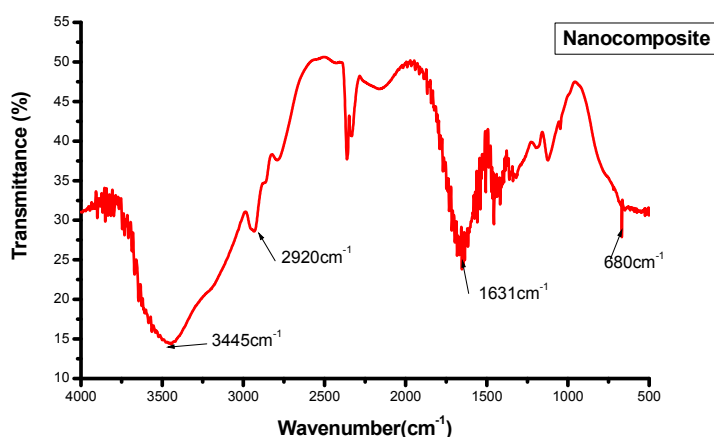


Figure 3.3 FTIR spectra of nanocomposite

### 3.3 Swelling measurement

#### 3.3.1 Kinetics study of swelling

The favourable property of hydrogels is their ability to swell, when put in contact with a thermodynamically compatible solvent. When a hydrogel in its initial state is in contact with solvent molecules, the latter attacks the hydrogel surface and penetrates into the polymeric network of the gels. The hydrogel containing 6.25 mg of magnetic crosslinker its swelling ratio is comparatively less than 3.12 mg magnetic crosslinker. And the highest swelling ratio shows the sample which is not contain of magnetic crosslinker. But it is rare, when we add less amount of crosslinker its swelling ratio is increasing than contain of without crosslinker based hydrogel. So we called our thesis work is unique. Again if we increasing magnetic crosslinker decreasing the swelling %.

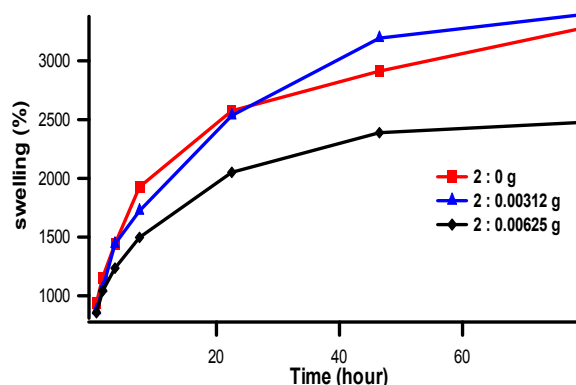


Figure 3.4 kinetics study of swelling

#### 3.3.2 Temperature dependent swelling study

The temperature dependent equilibrium swelling behavior of the hydrogels in deoxygenated distill water at a temperature range from 26 to 42°C. For this different concentration of  $Fe_3O_4$  cross-linkers were used and their roles on the swelling properties were examined. Increasing the temperature increased the swelling ratio. At 38°C decreased the swelling ratio of the hydrogel, which contain 6.25 mg, 3.12 mg magnetic crosslinker, and without crosslinker, decreased the swelling ratio at 34°C. Swelling behaviors of the hydrogel at different temperatures are shown in figure. If we increasing temperature, thermophilic hydrogel increasing its volume by include water



and if we increasing temperature thermophobic hydrogel decrease its volume by exclude water in the polymer chain. But at a significant temperature thermofillic hydrogel maintain collapse conformation by exclude water and thermophobic hydrogel maintain swelling conformation by include water. Our magnetic crosslinker based nanocomposite hydrogels significant temperature is 38°C. At this temperature, our magnetic crosslinker based hydrogel maintain collapse conformation, decrease its volume and another all temperature maintain swelling conformation increase its volume.

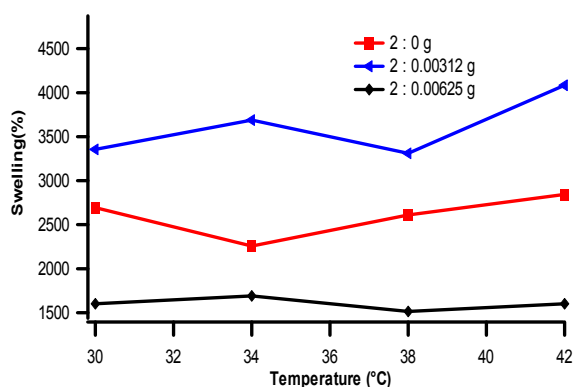


Figure 3.5 Temperature dependent swelling

### 3.4 Magnetic test of magnetic crosslinker and hydrogel

This test was performed two states like when the particles were in water and when the particles were dried. The magnetic test of the synthesized nanocomposite was carried out using magnetic bar. If the particles are magnetic then they are attracted by magnet and if the particles are not magnetic they are not attracted by the magnet. In the first case, the particles of our magnetic crosslinker which is dispersed in water strongly attracted by magnet. In the second case our magnetic crosslinker based nanocomposite hydrogel were in water but when a magnetic bar took to the vial then the particles were loosely attracted by the magnetic bar compare to our magnetic crosslinker. Because of our magnetic crosslinker based nanocomposite hydrogel also absorb a large amount of water and also create a big size. Our magnetic bar is not so strong as much as. So it is loosely attracted by the magnetic bar. Without magnetic crosslinker based hydrogel not attracted by the magnet. That is shown in figure.

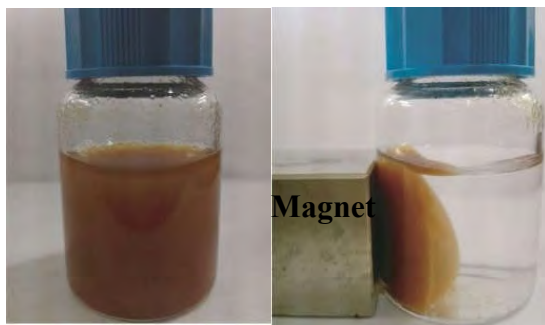


Figure 3.6 Magnetic crosslinker dispersed in water and get attract to magnet

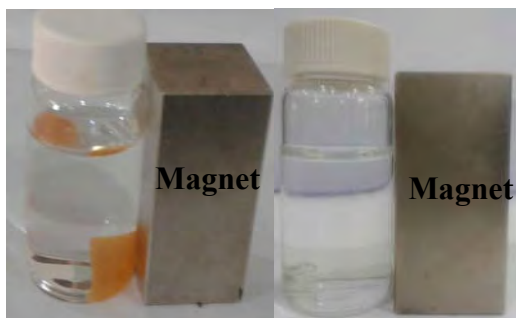


Figure 3.7 polymer nanocomposite hydrogel with magnetic crosslinker is attracted by magnet.

### 3.5 X-ray photoelectron spectroscopy (XPS)

We use the surface sensitive technique X-ray photoelectron spectroscopy (XPS) to conform the bonds that were formed in aminated MION, acrylated MION. The XPS spectra of aminated MION, acrylated MION is shown in Figure 3.8. In order to assess and confirm the bonds that were formed in aminated MION, acrylated MION, we use the most complicated, expensive and surface sensitive technique that is X-ray photoelectron spectroscopy.

From the Figure the XPS spectra of the two samples are similar because there is no elemental change occurred during aminated MION and the acrylation.

All XPS spectra of the presence of C1s, O1s, N1s, Si2s, Si2p. The spectrum of aminated MION the dominated species are O and Si. The species C and O are found at the binding energy 283.6eV and ~532.8eV, respectively. The intensity of N1s very small in aminated and acrylated MION. The presence of nitrogen on the surface was detected from its

characteristic emission peak at  $\sim 400\text{eV}$  and is due to the amination of silica coated MION and amide formation in acrylated MION.

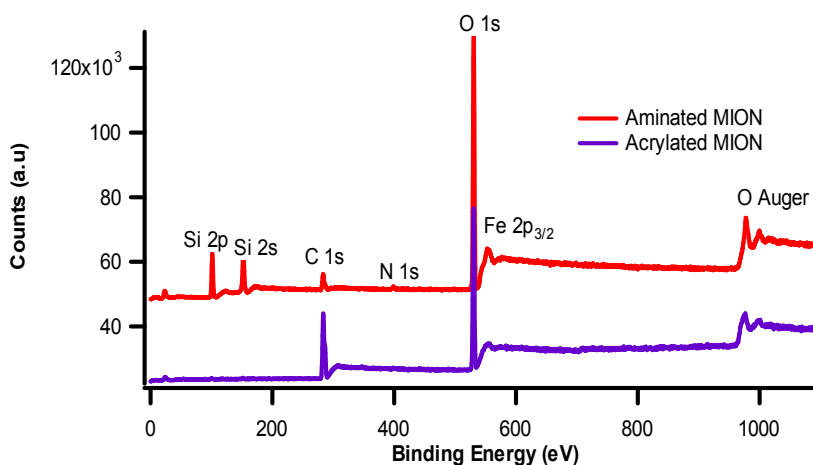


Figure 3.8 Widescanspectra of aminated MION, acrylated MION

The binding energy at  $100.4\text{eV}$  and  $151.2\text{eV}$  the existence of silicon on the surface as the magnetic iron oxide nanoparticles were coated with silica. All the two spectra have a common oxygen auger electron spectrum at binding energy  $978\text{eV}$ . Widescan spectra give idea about the elemental composition on the surface only. But their bonding nature could not be known by this spectrum.

### 3.5.1 High Resolution C1s Spectra

Widescan spectra showed the presence of C but the relation of C with other elements could not explain. For this high resolution of C1s spectra are taken. By this spectrum it is possible to know how the C bonded with other elements.

High resolution C1s spectra of aminated MION, are shown in figure 3.9. The C1s peak of aminated MION can be scattered into three components peak. According to the binding energy these peaks are assigned to the carbon of C-Si ( $284.3\text{eV}$ ), C-C ( $285.3\text{eV}$ ) and C-N ( $285.8\text{eV}$ ) [6-8, 9]. The binding energy  $284.5\text{eV}$  corresponds to a carbon atom bound only to silicon atom.

C-Si bond found due to the reaction between silanol groups of silica coated MION and 3-aminopropyltetraethylorthosilicate. Binding energy  $285.3$  ascribes to a carbon atom bound only to other carbon atoms and hydrogen atoms.  $285.8\text{eV}$  corresponds to a carbon

bound to single nitrogen atom. This is due to the terminal amino group linked with methylene group.

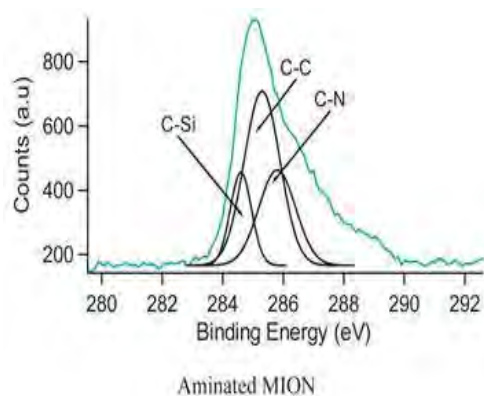


Figure 3.9 High resolution of C1s spectra of aminated MION

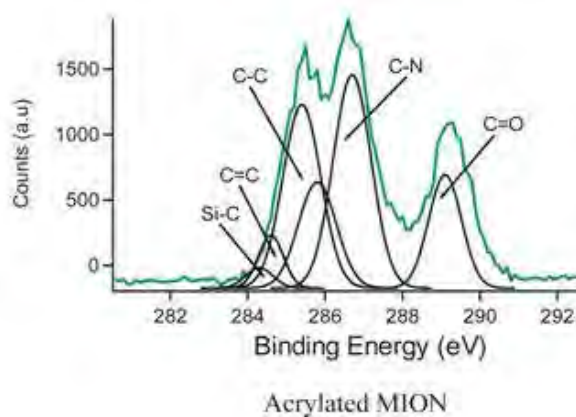


Figure 3.10 High resolution of C1s spectra of acrylated MION

After acrylation, there is significant changes appeared at the peak position. Now the peaks can be assigned into six components which are C-Si (284.3eV), C=C (284.6eV), C-C (285.4eV), N-C=O (286.6), C=O (288eV) and O-C=O (289.3eV) [10, 11]. An additional peak compare to aminated MION found at 284.6eV which ascribes the presence of C=C and it is the proof of the acrylation of the aminated MION. Another evidence for this is to the binding energy at 286.6eV for N-C=O which is mainly for the amide formation. The binding energy 289.3eV is due to the presence of O-C=O. This is most probably due to the presence of unreacted methacrylic anhydride.

### 3.5.2 High resolution N1s spectra

From the widescan spectrum it was seen that N was present but the bonding nature of N with other elements was unknown. The bonding nature of N with other elements high resolution of N1s spectra were carried out.

The high resolution N1s spectra of aminated MION are shown in Figure 3.11. In the case of aminated MION, there appears one peak at binding energy 400eV which describes the presence of primary amine at the end of chain.

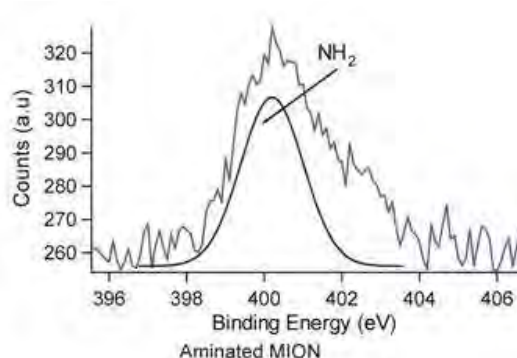


Figure 3.11 high resolution of N1s spectra of aminated MION

In the spectra of acrylated MION there are two scattered peaks appeared. First one is at binding energy 400eV and second one is for 402eV. Binding energy 400eV is attributed to a nitrogen atom linked to a carbon atom by a single bond (amide bond) [12], and the second peak at 402eV is assigned to the protonated amino group -NH<sub>3</sub><sup>+</sup> [13]. This indicates that all the amino groups in the aminated MION are not converted to amide.

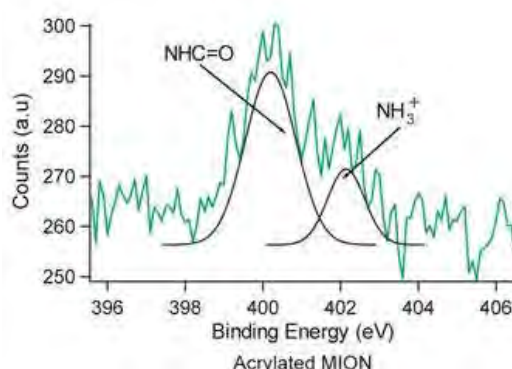


Figure 3.12 High resolution of N1s spectra of acrylated MION

### 3.6 X-ray diffraction analysis (XRD)

The crystalline properties and phase identification were characterized by X-ray diffraction using a Philips X'pert PRO X-ray diffractometer. The diffractogram was obtained by using Cu-K $\alpha$  radiation ( $\lambda = 0.15406\text{nm}$ ) in the range 10 to 70 $^{\circ}$  with steps of 0.021 and acquisition time of 1.0s/step.

The X-ray diffraction patterns of Fe<sub>3</sub>O<sub>4</sub> and nanocomposite were shown in figure 3.13.

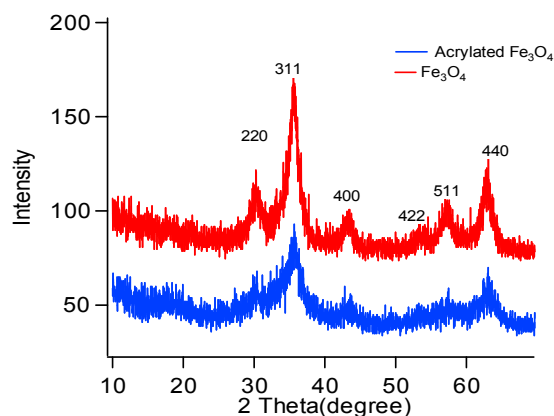


Figure 3.13 XRD spectra of Fe<sub>3</sub>O<sub>4</sub>, acrylated MION

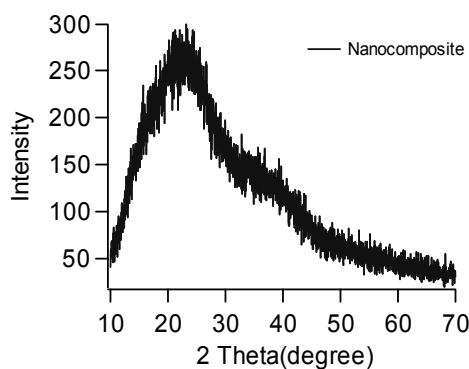


Figure 3.14 XRD spectra of nanocomposite

The Fe<sub>3</sub>O<sub>4</sub> particles have six diffraction peaks at  $2\theta = 30.24^{\circ}$ ,  $35.56^{\circ}$ ,  $43.38^{\circ}$ ,  $53.88^{\circ}$ ,  $57.34^{\circ}$ , and  $62.82^{\circ}$ . The peaks are associated with the crystallographic planes or Miller indices of (220), (311), (400), (422), (511), (440), respectively. It can be seen that, the peak position and relative intensities of the diffraction peaks are consistent with the characteristic peaks of standard Fe<sub>3</sub>O<sub>4</sub> crystal [Joint Committee on Powder Diffraction Standards (JCPDS card No.19-0629)] [14, 15]. The diffraction peaks of Fe<sub>3</sub>O<sub>4</sub> were indexed cubic spinel structure.

Nanocomposite samples did not exhibit any sharp peaks in XRD patterns, with only a broad peak at  $\sim 20^\circ$  attributed to the polymer networks.

From XRD data the average crystallite size was determined by Debye-Scherrer equation [16].

$$D_{hkl} = \frac{0.9\lambda}{\beta \cos\theta}$$

Where  $D_{hkl}$  is the average crystallite size,  $\lambda = 0.15406$  nm corresponds to the wavelength of Cu  $K\alpha$  radiation and  $\beta_{hkl}$  is full width half maximum (FWHM) in the  $2\theta$  scale of the diffraction peak from (hkl) crystal planes, and  $\theta$  is the Bragg angle. The crystallite size was determined by taking the average of the sizes at the peaks  $D_{220}$ ,  $D_{311}$ ,  $D_{400}$ ,  $D_{422}$ ,  $D_{511}$  and  $D_{440}$  and it was found to be about 5.32nm. The lattice parameter, “a” was determined by the following equation

$$d_{hkl} = \frac{a}{\sqrt{h^2 + l^2 + k^2}}$$

Where d = interplanar spacing

The lattice parameter was found to be 8.36 Å, which is lower than the values reported JCPDS card No. 19-629(a=8.39), but the value is very close to the theoretical value [17, 18, 19]. The lattice strain was also determined as 0.0237. The second XRD pattern for the acrylic modified  $Fe_3O_4$  and from the x-ray diffractogram found that peak position is remained same and it is the evident that there is no phase change occurred. The 3<sup>rd</sup> XRD pattern is for nanocomposite. From the pattern it is seen that, the nanocomposite has no sharp peak but at  $20^\circ$  attributed to the polymer networks.

### 3.7 Surface morphology study using scanning electron microscope (SEM)

Surface morphology of synthesized magnetic iron oxide nanoparticles (MION), acrylated MION and magnetic crosslinker based nanocomposite was studied by FE-SEM.

FE-SEM of magnetic iron oxide nanoparticle is shown below:

From figure 3.15 it is seen that particles of MION are spherical in shape and highly uniform in size. The average particle size is about 10-15nm. Some particles are very small and about 3-5nm and some particles aggregate due to large surface area and also magnetic attraction among them. From high resolution image it is clearly seen that particles are finely arranged.

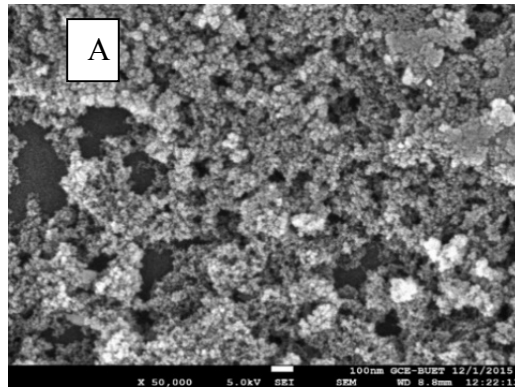


Figure 3.15 (A) SEM image of MION at Resolution x 50,000

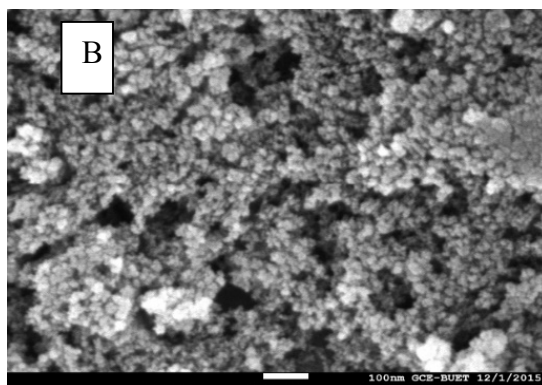


Figure3.15 (B) SEM image of (MION) at Resolution x 100,000.

Surface morphology of silica coated MION characterized by FE-SEM and the image shown in the figure3.16

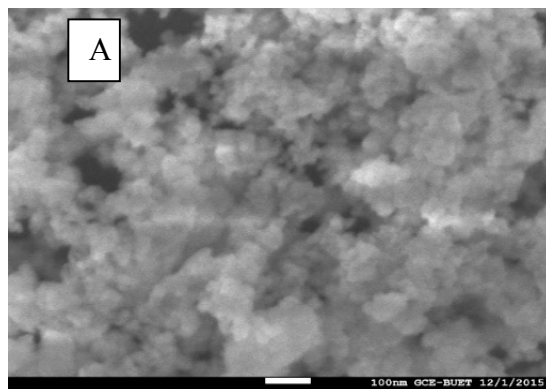


Figure 3.16 (A) SEM image of Silica coated MION at Resolution x 50,000



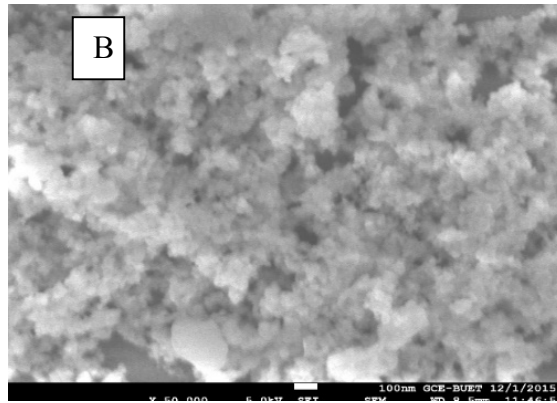


Figure 3.16 (B) SEM image of Silica coated MIONat Resolution x 100,000.

From the figure 3.16 it is seen that the average size of silica coated MION is about 15-20 nm.

Surface morphology of acrylated MION characterized by FE-SEM and the image shown in the figure3.16

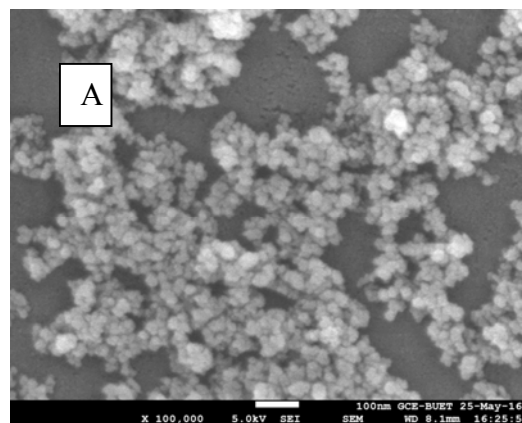


Figure3.17 (A)SEM image of acrylated MION (A) Resolution x 100,000

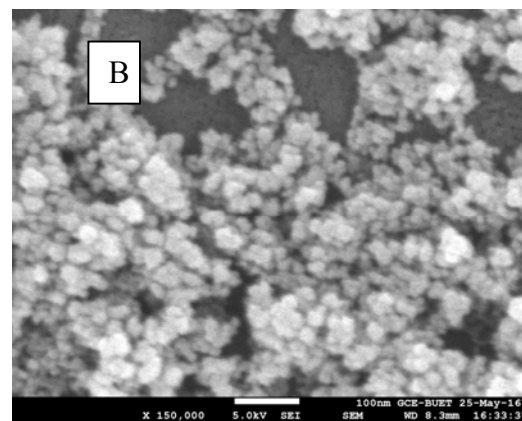


Figure3.17 (B)SEM image of acrylated MION (A) Resolution x 150,000

From the figure 3.17 it is seen that particles of acrylated MION are cubic in shape and size is about 20-30nm. Particles are randomly arranged and also seen that they are on one another. The shape of the particles is all most similar which are seen from the high resolution image.

FE-SEM image of nanocomposite is shown in the following figure

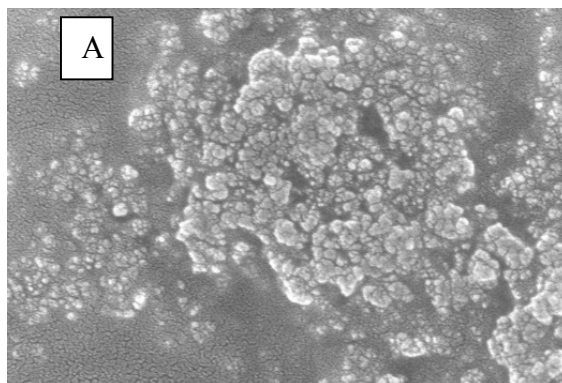


Figure 3.18 (A) SEM image of nanocomposite (4:0.025 g) at Resolution x 50,000

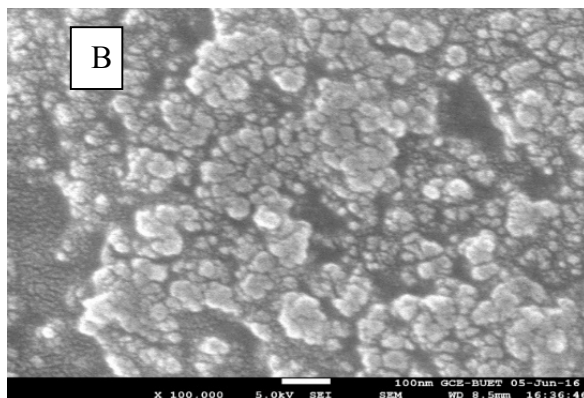


Figure 3.18 (B) SEM image of nanocomposite at Resolution x 100,000.

This nanocomposite contains 25 mg of acrylated MION that mean our targeted magnetic crosslinker which is magneto- and thermo- responsive nanocomposite hydrogel. Here acrylamide and magnetic crosslinker ratio is 4:0.025 g. The diameter of the nanocomposite is around to 70- 80 nm. The another nanocomposite which contain 12.5 mg of acrylated MION (magnetic crosslinker) that's ratio is 4:0.0125 g figure is given below. If we compare the SEM image of nanocomposite 4:0.125 g and 4:0.025 g. We increase the magnetic crosslinker also its shows densely. If we decrease the magnetic crosslinker the

nanaocomposite (4:0.0125 g) show less densely than 4:0.025 g. Less amount of crosslinker based nanocomposite (4:0.0125 g) SEM image is given below.

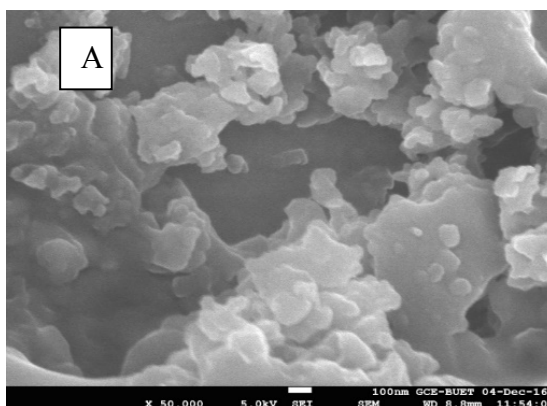


Figure 3.19 (A) SEM image of nanocomposite (4: 0.0125 g) at Resolution x 50,000

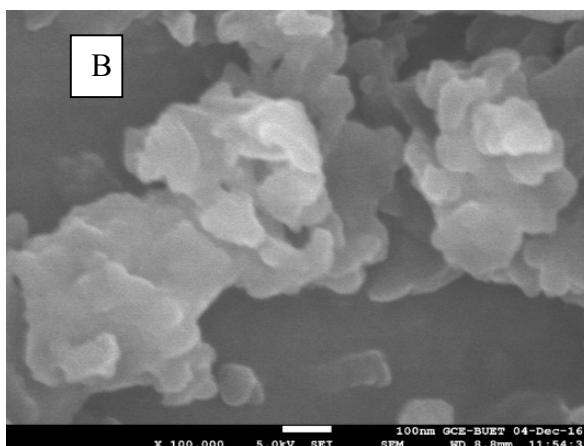


Figure 3.19 (B) SEM image of nanocomposite(4: 0.0125 g)at Resolution x 100,000.

### 3.8 Energy dispersive x-ray spectral analysis

Elemental analyses of the  $\text{Fe}_3\text{O}_4$ , silica coated MION, acrylated MION and nanocomposite have been performed by Energy Dispersive X-ray (EDX) method. The EDX patterns are presented in Figure 3.20-23. The peaks observed at 0.277, 0.392, 0.525, 1.739 and 6.398 keV, for K lines of C, N, O, Si and Fe respectively. The percentages of Fe, O, Si, N, and C were determined from the intensity of the lines and are summarized in Table 3.2.

From EDX analysis we found mass% of the composition and atom% of the composition.

Table 3.2 Elemental composition of magnetic and nanocomposite compound

Sample	Iron (Fe) %	Oxygen (O) %	Silicon (Si)%	Nitrogen (N)%	Carbon (C)%
Fe <sub>3</sub> O <sub>4</sub> (MION)	31	69			
Silica coated MION	14	42	43		
Acrylated MION	25	40	12	4	19
Nanocomposite	1	42	18	3	34

From the table it is seen that Fe<sub>3</sub>O<sub>4</sub> has iron content 31% and oxygen content 69%. It is approximately equal to the theoretical value of Fe<sub>3</sub>O<sub>4</sub>.

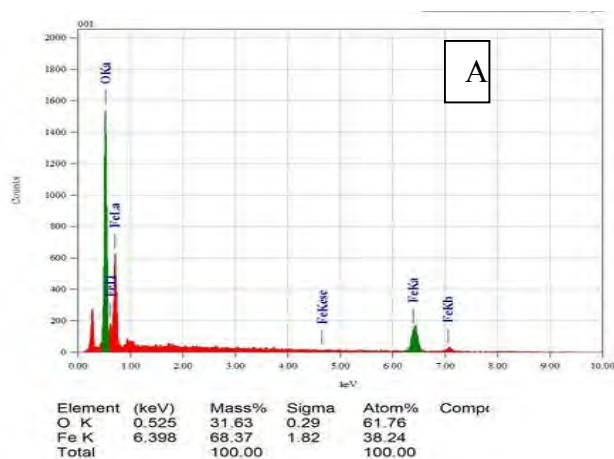


Figure 3.20 EDX spectra of Fe<sub>3</sub>O<sub>4</sub>

After silica coated of MION we expect we found a new element of Si, here we also found Si that is shown figure 3.21

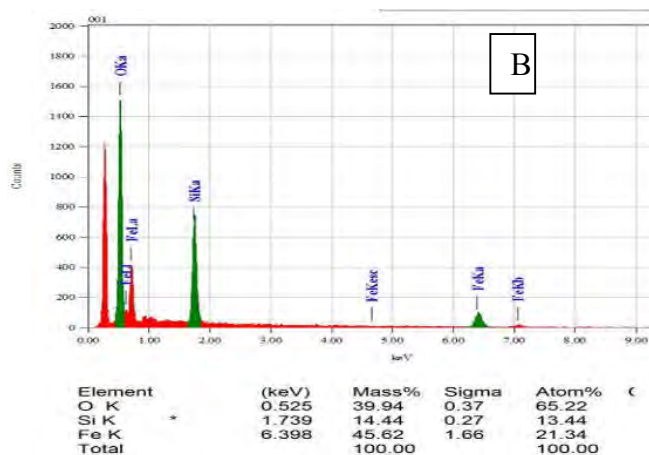


Figure 3.21 EDX spectra of silica coated of MION

After acrylation we found acrylated MION and here we expect that two new element are found because of aminated MION and acrylate MION. For this we found as a new element C and N and we also found this. So our targeted all element are found by EDX analysis

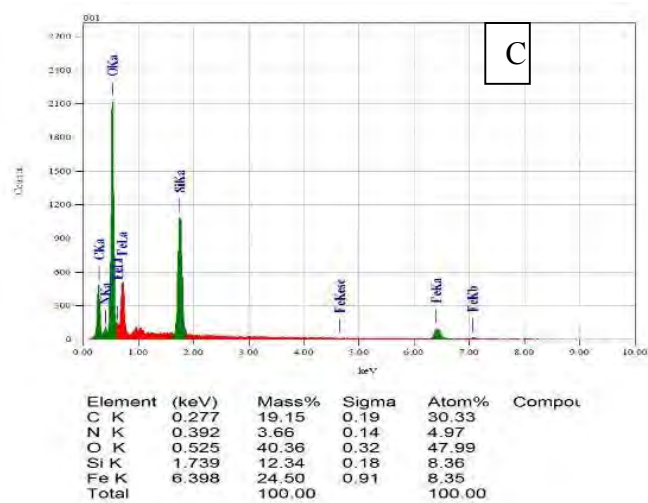


Figure 3.22 EDX spectra of acrylated MION

We synthesized different ratios of our magnetic crosslinker based hydrogel. This are 4:0.0125 g, 4:0.025. For this we found Fe and O amount are different. When we use 12 mg magnetic crosslinker then we found mass% of Fe 0.78 and O 34.07. Besides this when we use 25 mg of magnetic crosslinker we found mass% of Fe 1.05, O 42.44. This indicates when we increase magnetic crosslinker increase the mass% of Fe and O. EDX spectra of nanocomposite is given below

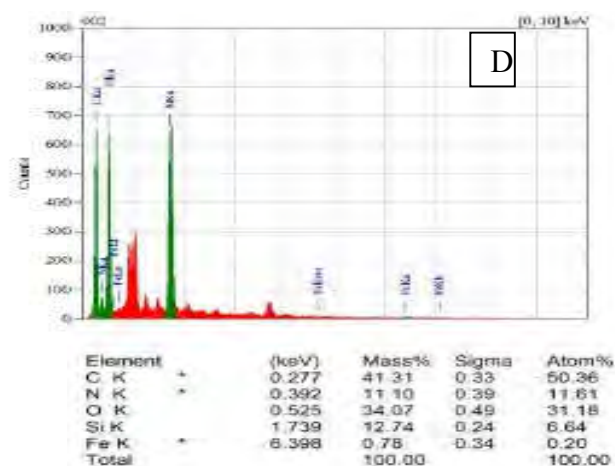


Figure 3.23 (A) EDX spectra of nanocomposite (4:0.0125g)

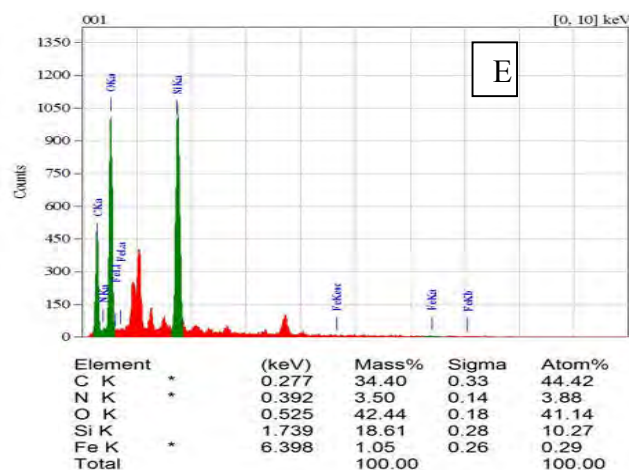


Figure 3.23 (B) EDX spectra of nanocomposite (4:0.025g)

### 3.9 Self-healing analysis

The magnetic hydrogel is self-healable, which is proven by the phenomenon shown in Fig 3.24. A piece of the original hydrogels was divided into two pieces using scissors and placed together immediately to insure contact of the freshly created fracture surfaces. After 1 h, the self-healing hydrogel was stretched to testing by hand. The hydrogels have excellent self-healing performance. Our magnetic nanocomposite based hydrogel contain  $\text{Fe}_3\text{O}_4$  nanoparticle. For this magnetic nanoparticle have particle-particle interaction and our magnetic crosslinker also have strong covalent bond. We use less amount of magnetic

nanoparticle than literature review, but our magnetic crosslinker based hydrogel show self-healing.

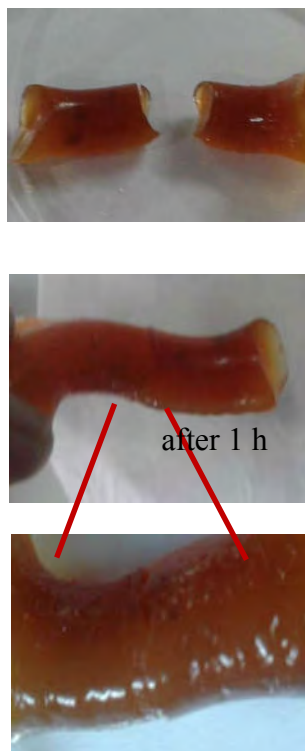


Figure3.24Fe<sub>3</sub>O<sub>4</sub>/PAAmhydrogel shows self-healing performance

## Conclusion

In this study, we synthesized magneto-and thermo-responsive superabsorbent nanocomposite hydrogel by using a magnetic crosslinker. We have introduced magnetic Fe<sub>3</sub>O<sub>4</sub> nanoparticles into the hydrogel system and these nanoparticles confirm by SEM and XRD analysis where the nanoparticle size is uniform in size. Our targeted magnetic crosslinker as characterized by FTIR and XPS analysis revealed that acrylic groups (-NHCOCH<sub>3</sub>CH=CH<sub>2</sub>) were successfully covalently bonded to the silica-coated Fe<sub>3</sub>O<sub>4</sub>. The elemental composition found by EDX and XPS supports that the synthesized material was our desired crosslinker. The high resolution of C1s results showed the presence of C-Si, C-C, C-N, C=O, C=C functional groups in the synthesized crosslinker. The high resolution of N1s spectra results also ascribed the formation of amide bond between the amino group

of aminated MION and anhydride group of the methacrylic anhydride and confirmed that the formation of magnetic crosslinker. Next, we performed an in situ polymerization of acrylamide in presence of the acrylated MION crosslinker using KPS initiator and employed FTIR, SEM, EDX and XRD for characterizing the synthesized nanocomposite hydrogel. The nanocomposite hydrogel exhibited excellent magnetic behavior confirming that our magnetic nanocomposite hydrogels are magneto- responsive. On the other hand, the swelling of the nanocomposite hydrogel was found to be temperature dependent, which proved the thermo-responsive nature. From the kinetics study of swelling we assured that if increasing magnetic crosslinker density decrease the swelling ratio. Besides, we did self-healing test on our hydrogel and found that the synthesized  $\text{Fe}_3\text{O}_4/\text{PAAm}$  hydrogel possessed excellent self-healing performance without any external intervention.



## References

1. Xu, J., Ju, C., Sheng, J., Wang, F., Zhang, Q., Sun, G., Sun, M., “Synthesis and characterization of magnetic nanoparticles and its application in lipase immobilization”, *Bull. Korean Chem. Soc*, vol.34(8), pp. 2408-2412, (2013).
2. Diaz, J., Paolicelli, G., Ferrer, S., Comin, F. “Separation of the sp<sup>3</sup> and sp<sup>2</sup> components in the C1s photoemission spectra of amorphous carbon films.” *Phys. Rev. B*, vol.54, pp. 8064-8069, (1996).
3. Li, Q. X., Wen, J. Y., Neoh, K. G., Kang, E. T., Guo, D. F., “Highly compressible and stretchable superhydrophobic coating inspired by bioadhesion of marine mussels.” *Macromolecules*, vol. 43, pp. 8336-8344, (2010).
4. Gao, H. C.; Sun, Y. M.; Zhou, J. J.; R. X.; Duan, H. W.; “Mussel-Inspired Synthesis of Polydopamine-Functionalized Graphene Hydrogel as Reusable Adsorbents for Water Purification.” *Acs Appl. Mater. Interfaces*, 2013, vol.5, pp.425-432 (2013).
5. Atta, A. M., El mahady, G. A., Al-Lohedan, H. A., Al Hussain, S. A., “Corrosion inhibition of a nanocomposite based on acrylamide copolymers /magnetite for steel.” *Digest Journal of Nanomaterials and Biostructures* vol. 9, pp. 627 – 639, (2014).
6. Bashouti, M. Y., Garzuzi, C. A., de la Mata, M., Arbiol, J., Ristein, J., Haick, H., Christiansen, S., “Role of Silicon Nanowire Diameter for Alkyl (Chain Lengths C1–C18) Passivation Efficiency through Si–C Bonds”, *Langmuir*, 2015, vol.31, pp. 2430–2437 (2015).
7. Jansen, R. J. J., Van Bekkum, H., “XPS of nitrogen-containing functional groups on activated carbon”, *Carbon*, vol. 33, pp. 1021–1027, (1995).
8. Zubavichus, Y., Zharnikov, M., Shaporenko, A., Fuchs, O., Weinhardt, L., Heske, C., Umbach, E., Denlinger, J. D., Grunze, M., “Soft X-ray induced

- decomposition of phenylalanine and tyrosine: A comparative study”, *J. Phys. Chem. A*, vol. 108, pp. 4557–4565, (2004).
9. He, Y. P.; Wang, S. Q.; Li, C. R.; Miao, Y. M.; Wu, Z. Y.; Zou, B. S.; “Synthesis and characterization of functionalized silica-coated Fe<sub>3</sub>O<sub>4</sub> superparamagnetic nanocrystals for biological applications.” *J. Phys. D: Appl. Phys.*, vol. 38, pp. 1342–1350 (2005).
  10. Zhang, H.; Zhong, X.; Xu, J. J.; Chen, H. Y., “Fe<sub>3</sub>O<sub>4</sub>/Polypyrrole/Au Nanocomposites with Core/Shell/Shell Structure: Synthesis, Characterization, and Their Electrochemical Properties.” *Langmuir* 2008, vol. 24, pp. 13748–13752, (2008).
  11. Fang, M.; Strom, V.; Olsson, R. T.; Belova, L.; Rao, K. V.; “Different Storage Conditions Influence Biocompatibility and Physicochemical Properties of Iron Oxide Nanoparticles.” *Nanotechnology*, vol. 23, p. 14560 (2012).
  12. Silva, V. A. J., Andrae, P. L., Silva, M. P., Bustamante, C. A. D., Valladares, L. D. L. S., Aguiar, J. A., “Synthesis and characterization of Fe<sub>3</sub>O<sub>4</sub> nanoparticles coated with fucan polysaccharides.” *Journal of Magnetism and Magnetic Materials*, Vol. 343, pp. 138–143, (2013).
  13. Khatiri, R., Reyhani, A., Mortazavi, S. Z., Hossainipour, M., “Preparation and characterization of Fe<sub>3</sub>O<sub>4</sub>/SiO<sub>2</sub>/ APTES core-shell nanoparticles.” *Proceedings of the 4<sup>th</sup> International Conference on Nanostructures (ICNS4)*, (2012).
  14. He, Y. P., Wang, S. Q., Li, C. R., Miao, Y. M., Wu, Z. Y., and Zou, B. S., “Synthesis and characterization of functionalized silica-coated Fe<sub>3</sub>O<sub>4</sub> superparamagnetic nanocrystals for biological applications.” *Journal of Physics. D: Applied. Physics*, vol. 38, pp 1342–1350 (2005).
  15. Ghasemzadeh, M. A., Basir, M. H. A., and Babaei, M., “Fe<sub>3</sub>O<sub>4</sub>@SiO<sub>2</sub>-NH<sub>2</sub> core-shell nanocomposite as an efficient and green catalyst for the multi-component synthesis of highly substituted chromenopyridines in aqueous ethanol media.” *Green Chemistry Letters and Reviews*, vol. 8, pp. 4–40, (2015).
  16. Zhou, X., Wang, J., Nie, J., and Du, B., “Poly(N-isopropylacrylamide)-based ionic hydrogels: synthesis, swelling properties, interfacial adsorption and release of dyes.” *Polymer Journal* vol. 48, pp. 431–438, (2016)

17. Chiu, W. S., Radiman, S., Abdullah, M. H., Khiewb, P. S., N.M. Huang, N. M., Abd-Shukor, R., “One pot synthesis of monodisperse Fe<sub>3</sub>O<sub>4</sub> nanocrystals by pyrolysis reaction of organometallic compound.” *Materials Chemistry and Physics* vol.106,pp. 231–235, (2007).
18. Liu, Y., Gao, Z. F., Sun, Q., Y. P. Zeng, Y. P., “The structure-tunable synthesis and magnetic properties of Fe<sub>3</sub>O<sub>4</sub> nanocrystals.” *Springer* vol. 219, pp. 107-112, (2013).
19. Liang, Y.; Xia, X.; Luo, Y.; Jia, Z.; “Synthesis and performances of Fe<sub>2</sub>O<sub>3</sub>/PA-6 nanocomposite fiber”, *Mater. Lett.* vol. 61, pp. 3269–3272, (2007).
20. Dubrovskii, S. A., Afanas’eva, M. V., Lagutina, M. A., and Kazanskii, K. S., “Measurement of swelling in weakly crosslinked hydrogels.” *Polymer Science U.S.S.R.* vol. 32, pp. 166-171, (1990).
21. Cao, S.; Li, X.; Lou, W.; Zong, M.; “Preparation of a novel magnetic cellulose nanocrystal and its efficient use for enzyme immobilization”, *J. Mater. Chem.* vol.2 (34), pp. 5522-5530, (2007).
22. Baker, J. P., D. R. Stephens, D. R., Blanch, H. W., and J. M. Prausnitz, J. M., “Swelling Equilibria for Acrylamide-Based Polyampholyte Hydrogels.” *ACS publications Macromolecules* vol.25, pp. 1955-1958, (1992).
23. Bennour, S., Louzri, F., “Study of Swelling Properties and Thermal Behavior of Poly(N,N’-Dimethylacrylamide-co-Maleic Acid) Based Hydrogels.” *Advances in Chemistry* vol. 2014, pp.147398-147407, (2014).
24. Chavda, H., Patel, C. N., “Effect of crosslinker concentration on characteristics of superporous hydrogel.” *International Journal of Pharmaceutical Investing*, vol.1, pp. 17-21, (2011).
25. Rapado, M., Peniche, C., “Synthesis and characterization of pH and temperature responsive poly(2-hydroxyethyl methacrylate-co-acrylamide) hydrogels.” *Journal of polymers*, vol.25. p. 6, (2015).
26. Ling, Y., Lu, M., “Preparation and Characterization of pH and Temperature Dual Responsive-, Poly(N-isopropylacrylamide-co-itaconic acid) Hydrogels Using DMF and Water as Mixed Solvents.” *Polymer Journal*, vol. 40, pp. 592–600, (2008).
27. Chaki, S. H., Malek, T. J., Chaudhary, M. D., Tailor, J. P., and M. P. Deshpande, M. P., “Magnetite Fe<sub>3</sub>O<sub>4</sub> nanoparticles synthesis by wet

- chemical reduction and their characterization.” *Journal of Nanoscience Nanotechnology*. P.6, (2015).
28. Wilson, D., M.A. Langell, M. A., “XPS analysis of oleylamine/oleic acid capped Fe<sub>3</sub>O<sub>4</sub> nanoparticles as a function of temperature.” *Applied Surface Science*, vol. 2, pp. 27222-27230, (2014).
29. Ding, H. L., Zhang, Y. X., Wang, S., Xu, J.M., Xu, S.C., and Li, G.H., “Fe<sub>3</sub>O<sub>4</sub>@SiO<sub>2</sub> Core/Shell Nanoparticles: The Silica Coating Regulations with a Single Core for Different Core Sizes and Shell Thicknesses.” *Chemistry of Materials*. vol. 24 (23), pp. 4572–4580,(2012).
30. Yamashita, T., Hayes, P., “Analysis of XPS spectra of Fe<sup>2+</sup> and Fe<sup>3+</sup> ions in oxide materials.” *Applied Surface Science*, vol. 254pp. 2441–2449, (2008).
31. Zhanga, Y., Bin Yanga, B., Zhanga, X., Xua, L., Tao, L., Lia, S., and Wei, Y., “Magnetic Self-healing Hydrogel.” *The Royal Society of Chemistry*, (2012).
32. Mingsen, C., Gong, G., Zhou, L., Zhang, F., “Facile fabrication of a magnetic self-healing poly (vinyl alcohol) composite hydrogel.” *Royal Society of Chemistry Advances*, vol. 7, pp. 21476–21483, (2017).